Accelerated Projected Gradient Algorithms for Sparsity Constrained Optimization Problems

Jan Harold Alcantara
Academia Sinica
Taipei, Taiwan
jan.harold.alcantara@gmail.com

Ching-pei Lee
Academia Sinica
Taipei, Taiwan
leechingpei@gmail.com

Abstract

We consider the projected gradient algorithm for the nonconvex best subset selection problem that minimizes a given empirical loss function under an ℓ_0-norm constraint. Through decomposing the feasible set of the given sparsity constraint as a finite union of linear subspaces, we present two acceleration schemes with global convergence guarantees, one by same-space extrapolation and the other by subspace identification. The former fully utilizes the problem structure to greatly accelerate the optimization speed with only negligible additional cost. The latter leads to a two-stage meta-algorithm that first uses classical projected gradient iterations to identify the correct subspace containing an optimal solution, and then switches to a highly-efficient smooth optimization method in the identified subspace to attain superlinear convergence. Experiments demonstrate that the proposed accelerated algorithms are magnitudes faster than their non-accelerated counterparts as well as the state of the art.

1 Introduction

We consider the sparsity-constrained optimization problem in $\Re^n$:

$$\min_{w \in A_s} f(w), \tag{1}$$

where f is convex with L-Lipschitz continuous gradient, $s \in \mathbb{N}$, and A_s is the sparsity set given by

$$A_s \coloneqq \{w \in \Re^n : \|w\|_0 \leq s\}, \tag{2}$$

where $\|w\|_0$ denotes the ℓ_0-norm that indicates the number of nonzero components in w. We further assume that f is lower-bounded on A_s.

A classical problem that fits in the framework of (1) is the best subset selection problem in linear regression [6, 20]. Given a response vector $y \in \Re^m$ and a design matrix of explanatory variables $X \in \Re^{m \times n}$, traditional linear regression minimizes a least squares (LS) loss function

$$f(w) = \|y - Xw\|^2/2. \tag{3}$$

However, due to either high dimensionality in terms of the number of features n or having significantly fewer instances m than features n (i.e., $m \ll n$), we often seek a linear model that selects only a subset of the explanatory variables that will best predict the outcome y. Towards this goal, we can solve (1) with f given by (3) to fit the training data while simultaneously selecting the best-s features. Indeed, such a sparse linear regression problem is fundamental in many scientific applications, such as high-dimensional statistical learning and signal processing [22]. The loss in (3) can be generalized to the following linear empirical risk to cover various tasks in machine learning beyond regression

$$f(w) = g(Xw), \quad g(z) = \sum\nolimits_{i=1}^{m} g_i(z_i), \tag{4}$$

where g is convex. Such a problem structure makes evaluations of the objective and its derivatives highly efficient, and such efficient computation is a key motivation for our algorithms for (1).

36th Conference on Neural Information Processing Systems (NeurIPS 2022).

Related Works. The discontinuous cardinality constraint in (1) makes the problem difficult to solve. To make the optimization problem easier, a popular approach is to slightly sacrifice the quality of the solution (either not strictly satisfying the sparsity level constraint or the prediction performance is deteriorated) to use continuous surrogate functions for the ℓ_0-norm, which lead to a continuous nonlinear programming problem, where abundant algorithms are at our disposal. For instance, using a convex penalty surrogate such as the ℓ_1-norm in the case of LASSO [36], the problem (1) can be relaxed into a convex (unconstrained) one that can be efficiently solved by many algorithms. Other algorithms based on continuous nonconvex relaxations such as the use of smoothly clipped absolute deviation [15] and the minimax concave penalty [41] regularizers are also popular in scenarios with a higher level of noise and outliers in the data. However, for applications in which enforcing the constraints or getting the best prediction performance is of utmost importance, solving the original problem (1) is inevitable. (For a detailed review, we refer the interested reader to [11, Section 1].) Unfortunately, methods for (1) are not as well-studied as those for the surrogate problems. Moreover, existing methods are indeed still preliminary and too slow to be useful in large-scale problems often faced in modern machine learning tasks.

In view of the present unsatisfactory status for scenarios that simultaneously involve high-volume data and need to get the best prediction performance, this work proposes efficient algorithms to directly solve (1) with large-scale data. To our knowledge, all the most popular algorithms that directly tackles (1) without the use of surrogates involve using the well-known projected gradient (PG) algorithm, at least as a major component [10–13, 3].[1] [10] proved linear convergence of the objective value with the LS loss function (3) for the iterates generated by PG under a scalable restricted isometry property, which also served as their tool to accelerate PG. However, given any problem instance, it is hard, if not computationally impossible, to verify whether the said property holds. On the other hand, [11] established global subsequential convergence to a stationary point for the iterates of PG on (1) without the need for such isometry conditions, and their results are valid for general loss functions f beyond (3). While some theoretical guarantees are known, the practicality of PG for solving (1) remains a big problem in real-world applications as its empirical convergence speed tends to be slow. The PG approach is called iterative hard thresholding (IHT) in studies of compressed sensing [13] that mainly focuses on the LS case. To accelerate IHT, several approaches that alternates between a PG step and a subspace optimization step are also proposed [12, 3], but such methods mainly focus on the LS case and statistical properties, while their convergence speed is less studied from an optimization perspective. Recently, "acceleration" approaches for PG on general nonconvex regularized problems have been studied in [27, 37]. While their proposed algorithms are also applicable to (1), the obtained convergence speed for nonconvex problems is not faster than that of PG.

This work is inspired by our earlier work [1], which considered a much broader class of problems without requiring convexity nor differentiability assumptions for f, and hence obtained only much weaker convergence results, with barely any convergence rates, for such general problems.

Contributions. In this work, we revisit the PG algorithm for solving the general problem (1) and propose two acceleration schemes by leveraging the combinatorial nature of ℓ_0-norm. In particular, we decompose the feasible set A_s as the finite union of s-dimensional linear subspaces, each representing a subset of the coordinates $\{1, \ldots, n\}$, as detailed in (7) of Section 2. Such subspaces are utilized in devising techniques to efficiently accelerate PG. Our first acceleration scheme is based on a same-space extrapolation technique such that we conduct extrapolation only when two consecutive iterates w_{k-1} and w_k lie in the same subspace, and the step size for this extrapolation is determined by a spectral initialization combined with backtracking to ensure sufficient function decrease. This is motivated by the observation that for (4), objective and derivatives at the extrapolated point can be inferred efficiently through a linear combination of Xw_{k-1} and Xw_k. The second acceleration technique starts with plain PG, and when consecutive iterates stay in the same subspace, it begins to alternate between a full PG step and a truncated Newton step in the subspace to obtain superlinear convergence with extremely low computational cost. Our main contributions are as follows:

1. We prove that PG for (1) is globally convergent to a local optimum with a local linear rate, improving upon the sublinear results of Bertsimas et al. [11]. We emphasize that our framework, like [11], is applicable to general loss functions f satisfying the convexity and smoothness

[1] [17] proposed an algorithm for a similar optimization problem that minimizes $f(w) + C\|w\|_0$ for some $C > 0$. But whether it is equivalent to (1) is unclear because both problems are nonconvex, and for any prespecified sparsity level s, it is hard to find C that leads to a solution w^* with $\|w^*\|_0 = s$.

requirements, and therefore covers not only the classical sparse regression problem but also many other ones encompassed by the empirical risk minimization (ERM) framework.
2. By decomposing A_s as the union of linear subspaces, we further show that PG is provably capable of identifying a subspace containing a local optimum of (1). By exploiting this property, we propose two acceleration strategies with practical implementation and convergence guarantees for the general problem class (1). Our acceleration provides both computational and theoretical advantages for convergence, and can in particular obtain superlinear convergence.
3. In comparison with existing acceleration methods for nonconvex problems [27, 37], this work provides new acceleration schemes with faster theoretical speeds (see Theorems 3.2 and 3.3), and beyond being applied to the classical PG algorithm, those schemes can also easily be combined with existing accelerated PG approaches to further make them converge even faster.
4. Numerical experiments exemplify the significant improvement in both iterations and running time brought by our acceleration methods, in particular over the projected gradient algorithm by [11] as well as the accelerated proximal gradient method for nonconvex problems proposed by [27].

This work is organized as follows. We review the projected gradient algorithm and prove its local linear convergence and subspace identification for arbitrary smooth loss functions in Section 2. In Section 3, we propose the acceleration schemes devised through decomposing the constraint set in (1) into subspaces of $\Re^n$. Experiments in Section 4 then illustrate the effectiveness of the proposed acceleration techniques, and Section 5 concludes this work. All proofs, details of the experiment settings, and additional experiments are in the appendices.

2 Projected Gradient Algorithm

The *projected gradient algorithm* for solving (1) is given by the iterations

$$w^{k+1} \in T^{\lambda}_{\mathrm{PG}}(w^k) \coloneqq P_{A_s}(w^k - \lambda \nabla f(w^k)), \tag{5}$$

where $P_{A_s}(w)$ denotes the projection of w onto A_s, which is set-valued because of the nonconvexity of A_s. When f is given by (3), global linear convergence of this algorithm under a restricted isometry condition is established in [10]. For a general convex f with L-Lipschitz continuous gradients, that is,

$$\|\nabla f(w) - \nabla f(w')\| \le L\|w - w'\| \quad \forall w, w' \in \Re^n, \tag{6}$$

the global subsequential convergence of (5) is proved in [11], but neither global nor local rates of convergence is provided. In this section, we present an alternative proof of global convergence and more importantly establish its local linear convergence.

A useful observation that we will utilize in the proofs of our coming convergence results is that the nonconvex set A_s given by (2) can be decomposed as a finite union of subspaces in $\Re^n$:

$$A_s = \bigcup\nolimits_{J \in \mathcal{J}_s} A_J, \quad A_J \coloneqq \operatorname{span}\{e_j : j \in J\}, \quad \mathcal{J}_s \coloneqq \{J \subseteq \{1, 2, \ldots, n\} : |J| = s\}, \tag{7}$$

where e_j is the jth standard unit vector in $\Re^n$. Throughout this paper, we assume that $\lambda \in (0, L^{-1})$.

Theorem 2.1. *Let $\{w^k\}$ be a sequence generated by* (5)*. Then:*

(a) (Subsequential convergence) Either $\{f(w^k)\}$ is strictly decreasing, or there exists $N > 0$ such that $w^k = w^N$ for all $k \ge N$. In addition, any accumulation point w^* of $\{w^k\}$ satisfies $w^* \in P_{A_s}(w^* - \lambda \nabla f(w^*))$, and is hence a stationary point of (1)*.*

(b) (Subspace identification and full convergence) There exists $N \in \mathbb{N}$ such that

$$\{w^k\}_{k=N}^{\infty} \subseteq \bigcup\nolimits_{J \in \mathcal{I}_{w^*}} A_J, \qquad \mathcal{I}_{w^*} \coloneqq \{J \in \mathcal{J}_s : w^* \in A_J\}. \tag{8}$$

whenever $w^k \to w^*$. In particular, if $T^{\lambda}_{\mathrm{PG}}(w^*)$ is a singleton for an accumulation point w^* of $\{w^k\}$, then w^* is a local minimum for (1)*, $w^k \to w^*$, and* (8) *holds.*

(c) (Q-linear convergence) If $T^{\lambda}_{\mathrm{PG}}(w^*)$ is a singleton for an accumulation point w^* and $w \mapsto w - \lambda \nabla f(w)$ is a contraction over A_J for all $J \in \mathcal{I}_{w^*}$, then $\{w^k\}$ converges to w^* at a Q-linear rate. In other words, there is $N_2 \in \mathbb{N}$ and $\gamma \in [0, 1)$ such that

$$\left\|w^{k+1} - w^*\right\| \le \gamma \left\|w^k - w^*\right\|, \quad \forall k \ge N_2. \tag{9}$$

It is well-known that an optimal solution of (1) is also a stationary point of it [8, Theorem 2.2], and therefore (a) proves the global subsequential convergence of PG to candidate solutions of (1). Consider $z^* := w^* - \lambda \nabla f(w^*)$, and let τ be a permutation of $\{1, \ldots, n\}$ such that $z^*_{\tau(1)} \geq z^*_{\tau(2)} \geq \cdots \geq z^*_{\tau(n)}$. The requirement of $T^\lambda_{\rm PG}(w^*)$ being a singleton in Theorem 2.1 (b) then simply means the mild condition of $z^*_{\tau(s)} > z^*_{\tau(s+1)}$, which is almost always true in practice. The requirement for (c) can be fulfilled when f confined to A_J is strongly convex, even if f itself is not. This often holds true in practice when f is of the form (4) and we restrict s in (1) to be smaller than the number of data instances m, and is thus also mild. The existence of a stationary point can be guaranteed when $\{w^k\}$ is a bounded sequence, often guaranteed when f is coercive on A_J for each $J \in \mathcal{J}_s$.

In comparison to existing results in [11, 2, 14], parts (b) and (c) of Theorem 2.1 are new. In particular, part (b) provides a full convergence result that usually requires stronger regularity assumptions like the Kurdyka-Łojasiewicz (KL) condition [2, 14] (see also (21)) that requries the objective value to decrease proportionally with the minimum-norm subgradient in a neighborhood of the accumulation point, but we just need the very mild singleton condition right at the accumulation point only. Part (c) gives a local linear convergence for the PG iterates even if the problem is nonconvex, while the rates in [14] requires a KL condition and the rate is measured in the objective value.

The following result further provides rates of convergence of the objective values even without the conventional KL assumption. The first rate below follows from [24].

Theorem 2.2. *Let $\{w^k\}$ be a sequence generated by* (5)*. If $w^k \to w^*$, such as when $T^\lambda_{\rm PG}(w^*)$ is a singleton at an accumulation point w^* of* (5)*, then*

$$f(w^k) - f(w^*) = o(k^{-1}). \tag{10}$$

Moreover, under the hypothesis of Theorem 2.1 (c), the objective converges to $f(w^*)$ R-linearly, i.e.,

$$f(w^k) - f(w^*) = O(\exp(-k)). \tag{11}$$

By using Theorem 2.1, we can also easily get rates faster than (10) under a version of the KL condition that is easier to understand and verify than those assumed in existing works. In particular, existing analyses require the KL condition to hold in a neighborhood in $\Re^n$ of an accumulation point, but we just need it to hold around w^* within A_J for the restriction $f|_{A_J}$ for each $J \in \mathcal{I}_{w^*}$. These results are postponed to Theorem 3.2 in the next section as the PG method is a special case of our acceleration framework.

3 Accelerated methods

The main focus of this work is the proposal in this section of new techniques with solid convergence guarantees to accelerate the PG algorithm presented in the preceding section. Our techniques fully exploit the subspace identification property described by the inclusion (8), as well as the problem structure of (4) to devise efficient algorithms.

We emphasize that the two acceleration strategies described below can be combined together, and they are also widely applicable such that they can be employed to other existing algorithms for (1) as long as such algorithms have a property similar to (8).

3.1 Acceleration by extrapolation

Traditional extrapolation techniques are found in the realm of convex optimization to accelerate algorithms [9, 31] with guaranteed convergence improvements, but were often only adopted as heuristics in the nonconvex setting, until some recent works showed that theoretical convergence can also be achieved [27, 37]. However, unlike the convex case, these extrapolation strategies for nonconvex problems do not lead to faster convergence speed nor an intuitive reason for doing so. An extrapolation step proceeds by choosing a *positive* stepsize along the direction determined by two consecutive iterates. That is, given two iterates w^{k-1} and w^k, an intermediate point $z^k := w^k + t_k(w^k - w^{k-1})$ for some stepsize $t_k \geq 0$ is first calculated before applying the original algorithmic map ($T^\lambda_{\rm PG}$ in our case).[2]

[2] it is clear that if $t_k \equiv 0$, we reduce back to the original algorithm.

Another popular acceleration scheme for gradient algorithms is the spectral approach pioneered by [5]. They take the differences of the gradients and of the iterates in two consecutive iterations to estimate the curvature at the current point, and use it to decide the step size for updating along the reversed gradient direction. It has been shown in [39] that equipping this step size with a backtracking procedure leads to significantly faster convergence for proximal gradient on regularized optimization problems, which includes our PG for (1) as a special case.

To describe our proposed double acceleration procedure that combines extrapolation and spectral techniques, we first observe that all PG iterates lie on A_s, and that A_s can be finitely decomposed as (7). When two consecutive iterates lie on the same convex subspace A_J for some $J \in \mathcal{J}_s$, within these two iterations, we are actually conducting convex optimization. In this case, an extrapolation step within A_J is reasonable because it will not violate the constraint, and acceleration can be expected from the improved rates of accelerated proximal gradient on convex problems in [9, 32]. Judging from Theorem 2.1 (b), the corresponding J is also a candidate index set that belongs to $\mathcal{I}_{w^*}$, so extrapolation within A_J makes further sense. We set $t_k = 0$ to skip the extrapolation step if d^k is not a descent direction for f at w^k. Otherwise, we start from some $\hat{t}_k > 0$ decided by the curvature information of f, and then execute a backtracking linesearch along $d^k := w^k - w^{k-1}$ to set $t_k = \eta^i \hat{t}_k$ for the smallest integer $i \geq 0$ that provides sufficient descent

$$f(w^k + t_k d^k) \leq f(w^k) - \sigma t_k^2 \|d^k\|^2, \tag{12}$$

given parameters $\eta, \sigma \in (0, 1)$. We then apply (5) to $z^k = w^k + t_k d^k$ to obtain w^{k+1}.

For the spectral initialization $\hat{t}_k$ for accelerating the convergence, instead of directly using approaches of [5, 39] that takes the reversed gradient as the update direction, we need to devise a different mechanism as our direction d^k is not directly related to the gradient. We observe that for the stepsize

$$\alpha_k := \left\langle s^k, s^k \right\rangle / \left\langle s^k, r^k \right\rangle, \quad s^k := w^k - w^{k-1}, \quad r^k := \nabla f(w^k) - \nabla f(w^{k-1}) \tag{13}$$

used in [5], the final update $-\alpha_k \nabla f(w^k)$ is actually the minimizer of the following subproblem

$$\min_{d \in \Re^n} \quad \left\langle \nabla f(w^k), d \right\rangle + \|d\|^2/(2\alpha_k). \tag{14}$$

By juxtaposing the above quadratic problem and the upper bound provided by the descent lemma [7, Lemma 5.7], we can view α_k^{-1} as an estimate of the local Lipschitz parameter that could be much smaller than L but still guarantee descent of the objective. We thus follow this idea to decide $\hat{t}_k$ using such curvature estimate and the descent lemma by

$$\hat{t}_k = \operatorname*{arg\,min}_{t \geq 0} \ \left\langle \nabla f(w^k), t d^k \right\rangle + \left\| t d^k \right\|^2/(2\alpha_k) \quad \Leftrightarrow \quad \hat{t}_k = -\left\langle \alpha_k \nabla f(w^k), d^k \right\rangle / \left\| d^k \right\|^2. \tag{15}$$

Another interpretation of (13) is that $\alpha_k^{-1} I$ also serves as an estimate of $\nabla^2 f(w^k)$,[3] and the objective in (14) is a low-cost approximation of the second-order Taylor expansion of f. However, we notice that for problems in the form of (4) and with $d^k \in A_J$, the exact second-order Taylor expansion

$$f(w^k + t d^k) \approx f(w^k) + t \left\langle \nabla f(w^k), d^k \right\rangle + t^2 \left\langle \nabla^2 f(w^k) d^k, d^k \right\rangle / 2 \tag{16}$$

can be calculated efficiently. In particular, for (4) and any $d^k \in A_J$, we get from $X d^k = X_{:,J} d_J^k$:

$$\begin{aligned} \nabla f(w^k)^\top d^k &= \nabla g\left((X w^k)\right)^\top \left(X_{:,J} d_J^k\right), \\ \left\langle \nabla^2 f(w^k) d^k, d^k \right\rangle &= \left\langle (X_{:,J} d_J^k), \nabla^2 g\left((X w^k)\right) (X_{:,J} d_J^k) \right\rangle, \end{aligned} \tag{17}$$

which can be calculated in $O(ms)$ time by computing $X_{:,J} d_J^k$ first. This $O(ms)$ cost is much cheaper than the $O(mn)$ one for evaluating the full gradient of f needed in the PG step, so our extrapolation plus spectral techniques has only negligible cost. Moreover, for our case of $d^k = w^k - w^{k-1}$, we can further reduce the cost of calculate $X_{:,J} d_J^k$ and thus (17) to $O(m)$ by recycling intermediate computational results needed in evaluating $f(w^k)$ through $X_{:,J} d_J^k = X w^k - X w^{k-1}$. With such tricks for efficient computation, we therefore consider the more accurate approximation to let $\hat{t}_k$ be

[3] As ∇f is Lipschitz continuous, it is differentiable almost everywhere. Here, we denote by $\nabla^2 f(w^k)$ a generalized Hessian of f at w, which is well-defined for f with Lipschitz continuous gradient [19].

the scalar that minimizes the quadratic function on the right-hand side of (16) for problems in the form (4). That is, we use

$$\hat{t}_k := -\left\langle \nabla f(w^k), d^k \right\rangle / \left\langle \nabla^2 f(w^k) d^k, d^k \right\rangle. \tag{18}$$

Finally, for both (18) and (15), we safeguard $\hat{t}_k$ by

$$\hat{t}_k \leftarrow P_{[c_k \alpha_{\min}, c_k \alpha_{\max}]} \left(\hat{t}_k \right) \tag{19}$$

for some fixed $\alpha_{\max} \geq \alpha_{\min} > 0$, where

$$c_k := \left\| (\nabla f(w^k))_J \right\| / (\zeta_k \left\| d^k \right\|), \quad \zeta_k := -\left\langle d^k, \nabla f(w^k) \right\rangle / (\left\| d^k \right\| \left\| (\nabla f(w^k))_J \right\|) \in (0, 1]. \tag{20}$$

We also note that the low cost of evaluating Xd^k is also the key to making the backtracking in (12) practical, as each $f(w^k + \eta^i \hat{t}_k d^k)$ can be calculated in $O(m)$ time through linear combinations of Xw^k and Xd^k. The above procedure is summarized in Algorithm 1 with global convergence guaranteed by Theorem 3.1. In Theorem 3.2, we establish its full convergence as well as its convergence rates under a KL condition at w^*: there exists neighborhood $U \subset \Re^n$ of w^*, $\theta \in [0, 1]$, and $\kappa > 0$ such that for every $J \in \mathcal{I}_{w^*}$,

$$(f(w) - f(w^*))^\theta \leq \kappa \| (\nabla f(w))_J \|, \quad \forall w \in A_J \cap U. \tag{21}$$

We denote by n_k the number of successful extrapolation steps in the first k iterations of Algorithm 1. The part of $\theta \in [0, 1/2]$ with f being convex in the last item of Theorem 3.2 is directly from the result of [25].

Theorem 3.1. *Under the hypotheses of Theorem 2.1, any accumulation point of a sequence generated by Algorithm 1 is a stationary point.*

Theorem 3.2. *Consider either* (5) *or Algorithm 1 with $\eta, \sigma, \epsilon \in (0, 1)$, and $\alpha_{\max} \geq \alpha_{\min} > 0$, and suppose that there is an accumulation point w^* of the iterates at which the KL condition holds. Then $w^k \to w^*$. Moreover, the following rates hold:*

(a) If $\theta \in (1/2, 1)$: $f(w^k) - f(w^*) = O((k + n_k)^{-1/(2\theta - 1)})$.
(b) If $\theta \in (0, 1/2]$: $f(w^k) - f(w^*) = O(\exp(-(k + n_k)))$.
(c) If $\theta = 0$, or $\theta \in [0, 1/2]$ and f is convex: there is $k_0 \geq 0$ such that $f(w^k) = f(w^*)$ for all $k \geq k_0$.

We stress that convexity of f is not required in Theorems 3.1 and 3.2 except the second half of the last item of Theorem 3.2. There are several advantages of the proposed extrapolation strategy over existing ones in [27, 37]. The most obvious one is the faster rates in Theorem 3.2 over PG such that each successful extrapolation step in our method contributes to the convergence speed, while existing methods only provide the same convergence speed as PG. Next, existing strategies only use prespecified step sizes without information from the given problem nor the current progress, and they only restrict such step sizes to be within $[0, 1]$. Our method, on the other hand, fully takes advantage of the function curvature and can allow for arbitrarily large step sizes to better decrease the objective. In fact, we often observe $t_k \gg 1$ in our numerical experiments. Moreover, our acceleration techniques utilize the nature of (7) and (4) to obtain very efficient implementation for ERM problems such that the per-iteration cost of Algorithm 1 is almost the same as that of PG, while the approach of [27] requires evaluating f and ∇f at two points per iteration, and thus has twice the per-iteration cost.

A finite termination result similar to Theorem 3.2 (c) is presented in [29] under a Hölderian error bound that is closely related to the KL condition, but their result requires convexity of both the smooth term and the regularizer, so it is not applicable to (1) that involves a nonconvex constraint.

3.2 Subspace Identification

In line with the above discussion, we interpret (8) as a theoretical property guaranteeing that the iterates of the projected gradient algorithm (5) will eventually identify the subspaces A_J that contain a candidate solution w^* after a finite number of iterations. Consequently, the task of minimizing f over the nonconvex set A_s can be reduced to a convex optimization problem of minimizing f over A_J. Motivated by this, we present a two-stage algorithm described in Algorithm 2 that switches to a high-order method for smooth convex optimization after a candidate piece A_J is identified to

Algorithm 1: Accelerated projected gradient algorithm by extrapolation (APG)

Given an initial vector $w^0 \in \Re^n$ and parameters $\epsilon, \eta, \sigma \in (0,1)$, $\alpha_{\max} \geq \alpha_{\min} > 0$, $\lambda \in (0, 1/L)$.
for $k = 0, 1, 2, \ldots$ **do**
  if $k > 0$; *w^{k-1} and w^k activate the same A_J; and $\zeta_k \geq \epsilon$* **then**
    $d^k \leftarrow w^k - w^{k-1}$, and compute $\hat{t}_k$ from (19) with either (15) or (18)
    for $i = 0, 1, \ldots$ **do**
      $t_k \leftarrow \eta^i \hat{t}_k$
      if (12) *is satisfied* **then** $z^k \leftarrow w^k + t_k d^k$, and break
  else $z^k \leftarrow w^k$
  $w^{k+1} \leftarrow T^{\lambda}_{\mathrm{PG}}(z^k)$

obtain even faster convergence. Since ∇f is assumed to be Lipschitz continuous, the generalized Hessian of f exists everywhere [19], so we may employ a semismooth Newton (SSN) method [35] with backtracking linesearch to get a faster convergence speed with low cost (details in Appendix A). In particular, we reduce the computation costs by considering the restriction of f on the subspace A_J by treating the coordinates not in J as non-variables so that the problem considered is indeed smooth and convex. As we cannot know a priori whether I_{w^*} is indeed identified, we adopt the approach implemented in [26, 28, 23] to consider it identified when w^k activates the same A_J for long enough consecutive iterations. To further safeguard that we are not optimizing over a wrong subspace, we also incorporate the idea of [38, 4, 28, 23] to periodically alternate to a PG step (5) after switching to the SSN stage. A detailed description of this two-stage algorithm is in Algorithm 2.

In the following theorem, we show that superlinear convergence can be obtained for Algorithm 2 even if we take only one SSN step every time between two steps of (5), using a simplified setting of twice-differentiability. For our next theorem, we need to introduce some additional notations. Given any $w \in A_J$, we use $f_J(w_J) \coloneqq f(w)$ to denote the function of considering only the coordinates of w in J as variables and treating the remaining as constant zeros. We assume that the conditions of Theorem 2.1 (b) hold with $w^* \in A_s$, and that f is twice-differentiable around a neighborhood U of w^* with $\nabla^2 f_J$ Lipschitz continuous in U and $\nabla^2 f_J(w^*)$ positive definite for all $J \in \mathcal{I}_{w^*}$.

Theorem 3.3. *Suppose that starting after $k \geq N$ and $P_{A_s}(w^k) \subset U$, we conduct t Newton steps between every two steps of* (5) *for $t \geq 1$:*

$$w^{k,0} \in P_{A_s}(w^k),\ \begin{cases} J & \in \mathcal{I}_{w^{k,0}}, \\ w_i^{k,j+1} & = 0, \quad \forall i \notin J, \quad j = 1, \ldots, t-1, \\ w_J^{k,j+1} & = w_J^{k,j} - \nabla^2 f_J(w_J^{k,j})^{-1} \nabla f_J(w_J^{k,j}), \end{cases} \quad w^{k+1} \in T^{\lambda}_{\mathrm{PG}}(w^{k,t}). \tag{22}$$

Then $w^k \to w^*$ at a Q-quadratic rate.

In practice, the linear system for obtaining the SSN step is only solved inexactly via a (preconditioned) conjugate gradient (PCG) method, and with suitable stopping conditions for PCG and proper algorithmic modifications such as those in [40, 30], superlinear convergence can still be obtained easily. Interested readers are referred to Appendix A for a more detailed description of our implementation.

4 Experiments

In this section, we conduct numerical experiments to demonstrate the accelerated techniques presented in Section 3. We employ Algorithm 1 (APG) with (18) to accelerate PG, and further accelerate APG by incorporating subspace identification described in Algorithm 2, which we denote by APG+.[4] Comparisons with the extrapolated PG algorithm of Li and Lin [27], which we denote by PG-LL, are also presented. PG-LL is a state-of-the-art approach for nonconvex regularized optimization and thus suitable for (1). For f in (1), we consider both LS (3) and logistic regression (LR)

$$f(w) = \sum\nolimits_{i=1}^{m} \log\left(1 + \exp\left(-y_i x_i^\top w\right)\right) + \mu \|w\|^2/2, \tag{23}$$

[4] That is, if $Unchanged < S$ in Algorithm 2, we calculate z^k as in Algorithm 1

Algorithm 2: Accelerated projected gradient algorithm by subspace identification (PG+)

Given an initial vector $w^0 \in \Re^n$ and $S, t \in \mathbb{N}$. Set Unchanged $\leftarrow 0$.
for $k = 0, 1, 2, \ldots$ **do**
  if $k > 0$, *and* w^{k-1} *and* w^k *activate the same component of* A_s **then**
    Let $J \in \mathcal{J}_s$ correspond to the activated component
    Unchanged $\leftarrow$ Unchanged $+1$
  else Unchanged $\leftarrow 0$
  if *Unchanged* $\geq S$ **then**
    $y^k \leftarrow P_{A_J}(w^k)$ and use t steps of SSN described in Appendix A, starting from y^k, to find z^k that approximately minimizes $f|_{A_J}$
    if *SSN fails* **then** $z^k \leftarrow w^k$ and Unchanged $\leftarrow 0$.
  else $z^k \leftarrow w^k$
  $w^{k+1} \leftarrow T^{\lambda}_{\mathrm{PG}}(z^k)$

where $(x_i, y_i) \in \Re^n \times \{-1, 1\}$, $i = 1, \ldots, m$, are the training instances, and $\mu > 0$ is a small regularization parameter added to make the logistic loss coercive.

The algorithms are implemented in MATLAB and tested with public datasets in Tables 2 and 3 in Appendix B. All algorithms compared start from $w^0 = 0$ and terminate when the first-order optimality condition

$$\text{Residual}(w) := \|w - P_{A_s}(w - \lambda \nabla f(w))\| / (1 + \|w\| + \lambda \|\nabla f(w)\|) < \hat{\epsilon} \tag{24}$$

is met for some given $\hat{\epsilon} > 0$. More setting and parameter details of our experiments are in Appendix B.

Comparisons of algorithms for large datasets. To fit the practical scenario of using (1), we specifically selected high-dimensional datasets with n larger than m. We conduct experiments with various s to widely test the performance under different scenarios. In particular, we consider $s \in \{\lceil 0.01m \rceil, \lceil 0.05m \rceil, \lceil 0.1m \rceil\}$ on all data except for the largest dataset webspam, for which we set $s \in \{\lceil 0.001m \rceil, \lceil 0.005m \rceil, \lceil 0.01m \rceil\}$. The results of the experiment with the smallest s are summarized in Figure 1, and results of the other two settings of s are in Appendix C.

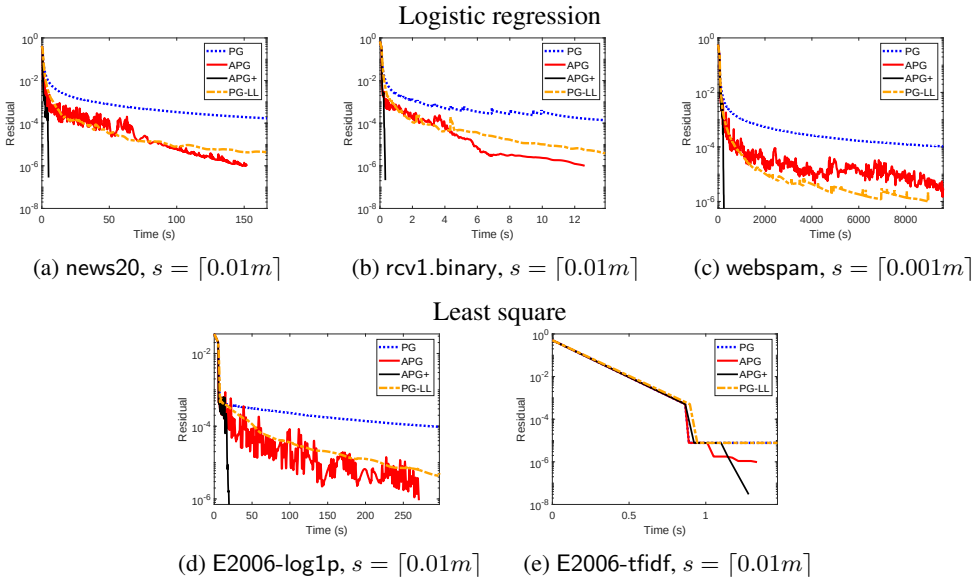

(a) news20, $s = \lceil 0.01m \rceil$ (b) rcv1.binary, $s = \lceil 0.01m \rceil$ (c) webspam, $s = \lceil 0.001m \rceil$

(d) E2006-log1p, $s = \lceil 0.01m \rceil$ (e) E2006-tfidf, $s = \lceil 0.01m \rceil$

Figure 1: Experiment on sparse regularized LR and LS. We present time v.s. residual in (24).

Evidently, the extrapolation procedure in APG provides a significant improvement in the running time compared with the base algorithm PG, and further incorporating subspace identification as in APG+ results to a very fast algorithm that outperforms PG and APG by magnitudes. Since the per-iteration

Table 1: Comparison of algorithms for (1) to meet (24) with $\hat{\epsilon} = 10^{-6}$, with (23) and (3) and with sparsity levels $s_1 = \lceil 0.01m \rceil$ and $s_2 = \lceil 0.05m \rceil$ for all datasets except webspam where $s_1 = \lceil 0.001m \rceil$ and $s_2 = \lceil 0.005m \rceil$. CPU: CPU time in seconds. GE: number of gradient evaluations. In one iteration, PG, APG, and APG+ needs one gradient evaluation , while PG-LL and PG-LL+ needs two. CG: number of Hessian-vector products in the PCG procedure for obtaining SSN steps. PA: prediction accuracy (for (23)). MSE: mean-squared error (for (3)). Time with $*$ indicates that the algorithm is terminated after running 10000 iterations without satisfying (24).

Dataset	Method	s_1				s_2			
		CPU	GE	CG	PA	CPU	GE	CG	PA
news20	PG	$*$738.7	10000	0	0.877	$*$728.9	10000	0	0.935
	APG	151.7	1583	0	0.877	758.3	8428	0	0.923
	APG+	**5.0**	52	63	0.853	**16.1**	171	67	0.923
	PG-LL	366.7	4682	0	0.873	$*$1494.4	20000	0	0.922
	APG-LL+	6.6	152	88	0.854	29.2	417	89	0.920
rcv1.binary	PG	$*$58.4	10000	0	0.937	$*$72.7	10000	0	0.951
	APG	12.6	1120	0	0.935	82.4	6372	0	0.934
	APG+	**0.3**	21	42	0.931	**2.4**	192	138	0.940
	PG-LL	22.2	3638	0	0.935	72.1	8738	0	0.929
	APG-LL+	0.6	99	49	0.930	4.9	626	236	0.939
webspam	PG	$*$18660.1	10000	0	0.964	$*$30776.2	10000	0	0.978
	APG	19683.4	7682	0	0.981	7722.4	2008	0	0.991
	APG+	**248.3**	75	88	0.969	**695.4**	164	57	0.991
	PG-LL	9001.3	4720	0	0.972	10163.5	3098	0	0.990
	APG-LL+	447.3	264	92	0.965	837.3	294	90	0.992
		CPU	GE	CG	MSE	CPU	GE	CG	MSE
E2006-log1p	PG	$*$2998.6	10000	0	0.167	$*$3644.1	10000	0	0.161
	APG	270.6	669	0	0.136	811.8	1757	0	0.133
	APG+	**19.5**	40	49	0.141	**105.6**	222	124	0.132
	PG-LL	$*$6049.8	20000	0	0.132	2696.0	7086	0	0.132
	APG-LL+	41.2	142	38	0.142	107.5	326	100	0.138
E2006-tfidf	PG	$*$242.7	10000	0	0.152	$*$666.9	10000	0	0.152
	APG	**1.3**	14	0	0.154	**3.3**	33	0	0.153
	APG+	**1.3**	8	6	0.141	**3.3**	31	7	0.139
	PG-LL	110.6	4440	0	0.152	304.8	4558	0	0.151
	APG-LL+	1.7	34	6	0.141	3.7	47	7	0.139

cost of PG and APG are almost the same as argued in Section 3, we note that the convergence of APG in terms of iterations is also superior to that of PG.

We also report the required time and number of gradient evaluations (which is the main computation at each iteration) for the algorithms to drive (24) below $\hat{\epsilon} = 10^{-6}$. For PG, APG, and APG+, one gradient evaluation is needed per iteration, so the number of gradient evaluations is equivalent to the iteration count. For PG-LL, two gradient evaluations are needed per iteration, so its cost is twice of other methods. We also report the prediction performance on the test data, and we in particular use the test accuracy for (23) and the mean-squared error for (3). Results for the two smaller s are in Table 1 while that for the largest s is in Appendix C. It is clear from the results in Table 1 that APG outperforms PG-LL for most of the test instances considered, while APG+ is magnitudes faster than PG-LL. When we equip PG-LL with our acceleration techniques by replacing $T_{\mathrm{PG}}^{\lambda}$ in Algorithms 1 and 2 with the algorithmic map defining PG-LL, we can further speed up PG-LL greatly as shown under the name APG-LL+ (see Table 1). We do not observe a method that consistently possesses the best prediction performance, as this is mainly affected by which local optima is found, while no algorithm is able to find the best local optima among all candidates. With no prediction performance degradation, we see that APG+ and APG-LL+ reduce the time needed to solve (1) to a level significantly lower than that of the state of the art.

In Appendix C.3, we demonstrate the effect on prediction performance when we vary the residual (24) and illustrate that tight residual level is indeed required to obtain better prediction. Comparisons with a greedy method is shown in Appendix C.4.

Transition Plots. To demonstrate the behavior of the algorithm for increasing values of s, we fit the smaller datasets in Table 3 using logistic loss (23) and least squares loss (3) for varying $s = \lceil km \rceil$, where $k = 0.2, 0.4, 0.6, \ldots, 3$. The transition plots are presented in Figure 2. We note that the time is in log scale.

We can see clearly that APG+ and APG-LL+ are consistently magnitudes faster than the baseline PG method throughout all sparsity levels. On the other hand, the same-subspace extrapolation scheme of APG is consistently faster than PG and APG-LL and slower than the two Newton acceleration schemes, although the performance is sometimes closer to APG+/APG-LL+ while sometimes closer to PG. APG-LL tends to outperform PG in most situations as well, but in several cases when solving the least square problem, especially when s is small, it can sometimes be slower than PG. Overall speaking, the results in the transition plots show that our proposed acceleration schemes are indeed effective for all sparsity levels tested.

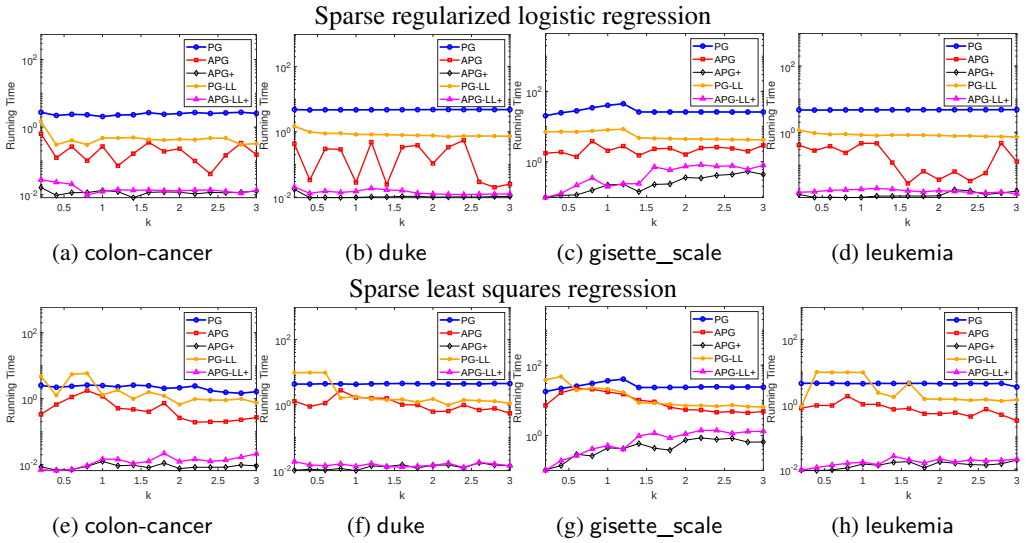

Figure 2: Transition plots. We present sparsity levels versus running time (in log scale). Top row: logistic loss. Bottom row: least square loss.

5 Conclusions

In this work, we revisited the projected gradient algorithm for solving ℓ_0-norm constrained optimization problems. Through a natural decomposition of the constraint set into subspaces and the proven ability of the projected gradient method to identify a subspace that contains a solution, we further proposed effective acceleration schemes with provable convergence speed improvements. Experiments showed that our acceleration strategies improve significantly both the convergence speed and the running time of the original projected gradient algorithm, and outperform the state of the art for ℓ_0-norm constrained problems by a huge margin. We plan to extend our analysis and algorithm to the setting of a nonconvex objective in the near future.

Acknowledgments

This work was supported in part by Academia Sinica Grand Challenge Program Seed Grant No. AS-GCS-111-M05 and NSTC of R.O.C. grants 109-2222-E-001-003 and 111-2628-E-001-003.

References

[1] Jan Harold Alcantara and Ching-pei Lee. Global convergence and acceleration of fixed point iterations of union upper semicontinuous operators: proximal algorithms, alternating and averaged nonconvex projections, and linear complementarity problems, 2022. arXiv:2202.10052. 2

[2] Hédy Attouch, Jérôme Bolte, and Benar Fux Svaiter. Convergence of descent methods for semi-algebraic and tame problems: proximal algorithms, forward–backward splitting, and regularized Gauss–Seidel methods. *Mathematical Programming*, 137(1):91–129, 2013. 4, 31, 32

[3] Sohail Bahmani, Bhiksha Raj, and Petros T. Boufounos. Greedy sparsity-constrained optimization. *Journal of Machine Learning Research*, 14:807–841, 2013. 2, 25

[4] Gilles Bareilles, Franck Iutzeler, and Jérôme Malick. Newton acceleration on manifolds identified by proximal-gradient methods. Technical report. arXiv:2012.12936. 7, 33

[5] Jonathan Barzilai and Jonathan M. Borwein. Two-point step size gradient methods. *IMA Journal of Numerical Analysis*, 8:141–148, 1988. 5

[6] E. M. L. Beale, M. G. Kendall, and D. W. Mann. The discarding of variables in multivariate analysis. *Biometrika*, 54(3-4):357–366, 1967. 1

[7] Amir Beck. *First-Order Methods in Optimization*. SIAM - Society for Industrial and Applied Mathematics, Philadelphia, PA, United States, 2017. 5, 27, 28

[8] Amir Beck and Yonina C. Eldar. Sparsity constrained nonlinear optimization: optimality conditions and algorithms. *SIAM Journal on Optimization*, 23(3):1480–1509, 2013. 4

[9] Amir Beck and Marc Teboulle. A fast iterative shrinkage thresholding algorithm for linear inverse problems. *SIAM Journal on Imaging Sciences*, 2(1):183–202, 2009. 4, 5

[10] Amir Beck and Marc Teboulle. A linearly convergent algorithm for solving a class of nonconvex/affine feasibility problems. In H. H. Bauschke, R. S. Burachik, P. L. Combettes, V. Elser, D. R. Luke, and H. Wolkowicz, editors, *Fixed-Point Algorithms for Inverse Problems in Science and Engineering*, volume 49 of *Springer Optimization and Its Applications*, pages 33–48. Springer, New York, NY, 2011. 2, 3

[11] D. Bertsimas, Angela King, and R. Mazumder. Best subset selection via a modern optimization lens. *Annals of Statistics*, 44(2):813–852, 2016. 2, 3, 4, 16

[12] Thomas Blumensath. Accelerated iterative hard thresholding. *Signal Processing*, 92:752–756, 2012. 2

[13] Thomas Blumensath and Mike E. Davies. Iterative hard thresholding for compressed sensing. *Applied and Computational Harmonic Analysis*, 27:265–274, 2009. 2

[14] Jérôme Bolte, Shoham Sabach, Marc Teboulle, and Yakov Vaisbourd. First order methods beyond convexity and lipschitz gradient continuity with applications to quadratic inverse problems. *SIAM Journal on Optimization*, 28(3):2131–2151, 2018. 4

[15] Jianqing Fan and Runze Li. Variable selection via nonconcave penalized likelihood and its oracle properties. *Journal of the American Statistical Association*, 96(456):1348–1360, 2001. 2

[16] Leonardo Galli and Chih-Jen Lin. A study on truncated newton methods for linear classification. *IEEE Transactions on Neural Networks and Learning Systems*, 2021. 15

[17] Jun-ya Gotoh, Akiko Takeda, and Katsuya Tono. DC formulations and algorithms for sparse optimization problems. *Mathematical Programming*, 169(1):141–176, 2018. 2

[18] Robert Hesse, D. Russell Luke, and Patrick Neumann. Alternating projections and Douglas-Rachford for sparse affine feasibility. *IEEE Trans. Signal Processing*, 62:4868–4881, 2014. 30

[19] Jean-Baptiste Hiriart-Urruty, Jean-Jacques Strodiot, and V Hien Nguyen. Generalized Hessian matrix and second-order optimality conditions for problems with $C^{1,1}$ data. *Applied Mathematics & Optimization*, 11(1):43–56, 1984. 5, 7, 14

[20] Ronald R. Hocking and R. N. Leslie. Selection of the best subset in regression analysis. *Technometrics*, 9(4):531–540, 1967. 1

[21] Chih-Yang Hsia, Wei-Lin Chiang, and Chih-Jen Lin. Preconditioned conjugate gradient methods in truncated newton frameworks for large-scale linear classification. In *Asian Conference on Machine Learning*, pages 312–326, 2018. 14

[22] Prateek Jain and Purushottam Kar. Non-convex optimization for machine learning. *Foundations and Trends in Machine Learning*, 10(3–4):142–363, 2017. 1

[23] Ching-pei Lee. Accelerating inexact successive quadratic approximation for regularized optimization through manifold identification. Technical report, 2020. arXiv:2012.02522. 7

[24] Ching-pei Lee and Stephen J. Wright. First-order algorithms converge faster than $O(1/k)$ on convex problems. In *Proceedings of the International Conference on Machine Learning*, 2019. 4, 29

[25] Ching-pei Lee and Stephen J. Wright. Revisiting superlinear convergence of proximal Newton methods to degenerate solutions. Technical report, 2022. 6, 33

[26] Sangkyun Lee and Stephen J. Wright. Manifold identification in dual averaging for regularized stochastic online learning. *Journal of Machine Learning Research*, 13:1705–1744, 2012. 7

[27] Huan Li and Zhouchen Lin. Accelerated proximal gradient methods for nonconvex programming. In *Advances in Neural Information Processing Systems*, volume 28, 2015. 2, 3, 4, 6, 7

[28] Yu-Sheng Li, Wei-Lin Chiang, and Ching-pei Lee. Manifold identification for ultimately communication-efficient distributed optimization. In *Proceedings of the 37th International Conference on Machine Learning*, 2020. 7

[29] Mingrui Liu and Tianbao Yang. Adaptive accelerated gradient converging method under Hölderian error bound condition. *Advances in Neural Information Processing Systems*, 30, 2017. 6

[30] Boris S. Mordukhovich, Xiaoming Yuan, Shangzhi Zeng, and Jin Zhang. A globally convergent proximal Newton-type method in nonsmooth convex optimization. *Mathematical Programming*, 2022. Online first. 7, 15

[31] Yurii Nesterov. A method for unconstrained convex minimization problem with the rate of convergence $o(1/k^2)$. *Soviet Mathematics Doklady*, 27(2):372–376, 1983. 4

[32] Yurii E. Nesterov. Gradient methods for minimizing composite functions. *Mathematical Programming*, 140(1):125–161, 2013. 5

[33] Jorge Nocedal and Stephen J. Wright. *Numerical Optimization*. Springer, New York, NY, USA, 2e edition, 2006. 14, 33

[34] Boris T. Polyak. *Introduction to Optimization*. Translation Series in Mathematics and Engineering. 1987. 32

[35] Liqun Qi and Jie Sun. A nonsmooth version of Newton's method. *Mathematical programming*, 58(1-3):353–367, 1993. 7

[36] Robert Tibshirani. Regression shrinkage and selection via the lasso. *Journal of the Royal Statistical Society Series B*, 58(1):267–288, 1996. 2

[37] Bo Wen, Xiaojun Chen, and Ting Kei Pong. A proximal difference-of-convex algorithm with extrapolation. *Computational Optimization and Applications*, 69:297–324, 2018. 2, 3, 4, 6

[38] Stephen J. Wright. Accelerated block-coordinate relaxation for regularized optimization. *SIAM Journal on Optimization*, 22(1):159–186, 2012. 7

[39] Stephen J. Wright, Robert D. Nowak, and Mário A. T. Figueiredo. Sparse reconstruction by separable approximation. *IEEE Transactions on Signal Processing*, 57(7):2479–2493, 2009. 5

[40] Man-Chung Yue, Zirui Zhou, and Anthony Man-Cho So. A family of inexact SQA methods for non-smooth convex minimization with provable convergence guarantees based on the Luo–Tseng error bound property. *Mathematical Programming*, 174(1-2):327–358, 2019. 7, 15

[41] Cun-Hui Zhang. Nearly unbiased variable selection under minimax concave penalty. *The Annals of Statistics*, 38(2):894–942, 2010. 2

Appendices

A Implementation Details for Section 3.2

We first discuss our implementation for obtaining inexact SSN steps described in Section 3.2. Given any $w \in A_J$, We use the notation $f_J(w_J) \coloneqq f(w)$ to denote the function of considering only the coordinates of w in J as variables and treating the remaining as constants equal to zero. For any $p \in \Re^s$, we use $P_{A_J}^{-1}$ to denote the vector $\hat{p} \in \Re^n$ with $\hat{p}_J = p$ and $\hat{p}_i = 0$ for $i \notin J$. Note that since f_J is Lipschitz-continuously differentiable, a generalized Hessian $\nabla^2 f_J$ always exists [19]. When the set of generalized Hessian is not a singleton, we can pick any element in the set.

In large-scale problems often faced in modern machine learning tasks, s can be large even if $s \ll n$, and thus forming the generalized Hessian explicitly and inverting it could still be prohibitively expensive even if we only consider the generalized Hessian in the s-dimensional subspace. Therefore, we resort to PCG that, given a preconditioner M, iteratively uses the matrix-vector products $\nabla^2 f_J(w_J)v$ and $M^{-1}u$ for given vectors $u, v \in \Re^s$, which can be of much lower cost especially if M has certain structures to facilitate the inverse. Details of PCG can be found in, for instance, Nocedal and Wright [33, Chapter 7]. The PCG approach provides an approximate solution to

$$p \approx \nabla^2 f_J(w_J)^{-1} \nabla f_J(w_J),$$

or equivalently,

$$p \approx \arg\min_{\bar{p}} \left(Q_J(\bar{p}; w_J) \coloneqq \langle \nabla f_J(w_J), \bar{p} \rangle + \frac{1}{2} \left\langle \bar{p}, \nabla^2 f_J(w_J) \bar{p} \right\rangle \right). \tag{25}$$

In our implementation, inspired by the approach of [21], we select the diagonal entries of $\nabla^2 f_J$ as our preconditioner M, which provides better performance in our preliminary test over using no preconditioner (or equivalently, taking M as the identity matrix). As this choice of M is a diagonal matrix, its inverse can be computed efficiently in $O(s)$ time.

After obtaining p, given parameters $\beta, \sigma_2 \in (0, 1)$, we conduct a backtracking line search procedure to find the largest nonnegative integer i such that

$$f_J\left(w_J + \beta^i p\right) \leq f_J\left(w_J\right) + \sigma_2 \beta^i \left\langle \nabla f_J\left(w_J\right), p \right\rangle \tag{26}$$

Table 2: Data statistics.

Dataset	Loss	#training instances (m)	#features (n)	#test instances
news20	(23)	15,997	1,355,191	3,999
rcv1.binary	(23)	20,242	47,236	677,399
webspam	(23)	280,000	16,609,143	70,000
E2006-log1p	(3)	16,087	4,272,227	3,308
E2006-tfidf	(3)	16,087	150,360	3,308

and set the step size to $\alpha = \beta^i$. Finally, the iterate is updated by

$$w_J \leftarrow w_J + \alpha p.$$

If α is too small, or this decrease condition cannot be satisfied even when β^i is already extremely small, we discard this SSN step and declare that this smooth optimization part has failed in Algorithm 2.

For the approximation criterion in (25), let the i-th iterate of PCG be $p^{(i)}$ and $Q_i \coloneqq Q_J(p^{(i)}; w_J)$, we follow [16] to terminate PCG either when it reaches s iterations (at which point theoretically it should have found the exact solution of the right-hand side of (25)) or when the i-th iterate satisfies $i \geq 1$ and

$$\frac{Q_i - Q_{i-1}}{\frac{Q_i}{i}} \leq \min\left\{0.5, \sqrt{\langle \nabla f_J(w_J), M^{-1}\nabla f_J(w_J)\rangle}\right\}, \tag{27}$$

where $Q_0 \coloneqq Q(0; w_J) = 0$. It has been shown in [16] that such a stopping condition leads to Q-superlinear convergence to an optimum of f_J when ∇f_J is semismooth and f is strongly convex. In our case that alternates between such an SSN step and a PG step, we will show that with (27), the overall procedure will enjoy superlinear convergence to w^* if ∇f is semismooth around x^*; see Theorem F.1 for more details.

One concern is that PCG only works when $\nabla^2 f_J$ is positive definite, but our problem class only guarantees that it is positive semidefinite. To safeguard this issue, one can add a multiple of the identity to $\nabla^2 f_J$ as a damping term to make sure the quadratic term is always positive definite. A particularly useful way is to use $c\|\nabla f_J(w_J)\|^\rho I$ as the damping term for some $c > 0$ and $\rho \in (0, 1]$ in (27). When f_J satisfies a q-metric subregularity condition or an error-bound condition, this damping is known to produce a superlinear convergence rate of order $(1 + \rho)$ for a range of q following the analysis in [40, 30]. In Theorem F.1, we do not consider any specific scenarios, but just assume that the smooth optimization subroutine involved itself has a superlinear convergence rate, and show that such a rate is still retained when this subroutine is combined with our algorithm. Therefore, discussions of various schemes including truncated Newton, semismooth Newton, and damping, are all compatible with our general framework to obtain superlinear convergence rates.

B Experimental settings

All experiments are conducted on a machine with 64GB memory and an Intel Xeon Silver 4208 CPU with 8 cores and 2.1GHz. For all algorithms and all experiments, all cores are utilized. The experiment environment runs Ubuntu 20.04 and MATLAB 2021b. For experiments in Section 4, we use public data listed in Tables 2 and 3. [5] For the datasets that do not come with a test set, we manually do a $80/20$ split to obtain a test set.

The parameters used in our implementation are as follows. We use $\mu = 10^{-10}$ in (23). For Algorithm 1, $\sigma = 0.05$, $\eta = 0.5$, $\epsilon = 10^{-20}$, $\alpha_{\min} = 1$, $\alpha_{\max} = 100$, L is estimated using MATLAB's `eigs` function to approximate the largest eigenvalue of AA^T with tolerance 10^{-3}, and $\lambda = 0.999/L$. In Algorithm 2, we set $t = 1$ and $S = 5$, while for the PCG and SSN subroutines, we set $\beta = 0.5$ and $\sigma_2 = 0.001$.

[5] Downloaded from `http://www.csie.ntu.edu.tw/~cjlin/libsvmtools/datasets/`.

Table 3: Data statistics for small datasets.

Dataset	Loss	#training instances (m)	#features (n)	#test instances
colon-cancer	(3)&(23)	50	2,000	12
duke	(3)&(23)	38	7,129	6
gisette_scale	(3)&(23)	1,000	5,000	6,000
leukemia	(3)&(23)	38	7,129	34

C Additional Experiments

This section provides two sets of additional experiments. We first present results of the datasets in Section 4 with different settings of s. The second set of additional experiments are on some smaller datasets that are often considered in existing works for the best subset selection problem like [11].

C.1 Other settings of s

We present the other two settings of s described in Section 4 in Figures 3 and 4, and the continuation of Table 1 is presented in Table 4. Additional experiments with the setting of $s > m$ are presented in Tables 5 and 6, which further exemplifies the benefits of our proposed acceleration strategies.

Clearly, for the setting of s_3 as well as $s > m$, our acceleration techniques continue to greatly improve upon existing methods in almost all cases, with the only excepion being webspam with $s > m$. After a thorough check, we found that the reason is that in this setting, due to the high dimensionality of n and that many pieces of $J \in \mathcal{J}_s$ can lead to a very low objective value, the subspaces in which each w^k lie change very frequently, so our extrapolation barely take place. This is a potential limit of our method, although in practice we observe that for such easier datasets we probably can avoid this problem by setting $s < m$, which would also make the problem much easier to solve in general (note that with $s < m$, the prediction performance on webspam is not improving at all, suggesting that indeed we do not need to consider the more difficult situation of $s < m$).

We also observe that all for $s \geq m$ on E2006-log1p, all accelerated methods experience significantly larger MSE than the base PG method. After a close examination, we find out that all such acceleration methods provide much lower objective value than PG for the minimization problem, indicating that this is merely due to overfitting of the training data, and indeed PG is alway terminated without reaching the prespecified stopping condition for these cases. This indicates that the accelerated methods are actually performing well from the optimization angle, and this overfitting issue is just a matter of parameter selection.

For E2006-tfidf, we see that for all settings of s, identification does not show any additional time improvement in the tables, while the figures clearly show that this is due to that this step kicks in at a very late stage when the residual is already very close to $\hat{\epsilon}$, and if we set $\hat{\epsilon}$ to a smaller value, we can expect observable running time difference between APG and APG+.

C.2 Experiments with smaller datasets

We now consider some other smaller datasets shown in Table 3, which are also downloaded from the LIBSVM website. Note that for gisette_scale, we interchanged the training and the test sets to make $m < n$. For the setting of $s < m$, we consider $s \in \{\lceil 0.01m \rceil, \lceil 0.05m \rceil, \lceil 0.1m \rceil, \lceil 0.5m \rceil\}$, while for the setting of $s \geq m$, we consider $s \in \{m, \lceil 1.1m \rceil, \lceil 1.5m \rceil, 2m\}$. The results of least-square loss in (3) are shown in Tables 7 and 8, while the results of the logistic loss in (23) are shown in Tables 9 and 10.

We can clearly see from these results that our acceleration schemes are also effective on smaller datasets to reduce the running time to magnitudes shorter. However, there are several cases that the running time is too short such that the digits in the tables are unable to show difference between APG and APG+. We do not try to increase the number of digits in such cases, as the running time is anyway already extremely short, and the difference would not make much difference for problems that can be solved with such high efficiency.

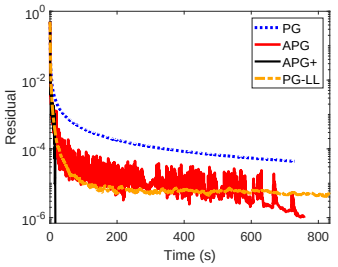

(a) news20, $s = \lceil 0.05m \rceil$

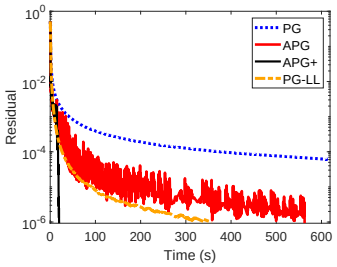

(b) news20, $s = \lceil 0.1m \rceil$

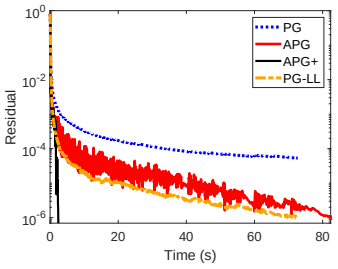

(c) rcv1.binary, $s = \lceil 0.05m \rceil$

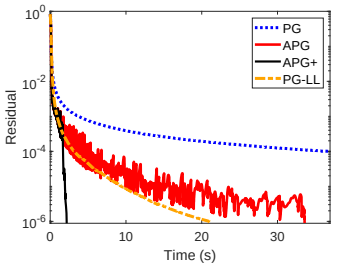

(d) rcv1.binary, $s = \lceil 0.1m \rceil$

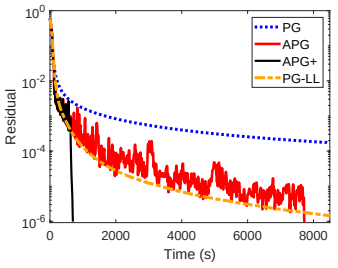

(e) webspam, $s = \lceil 0.005m \rceil$

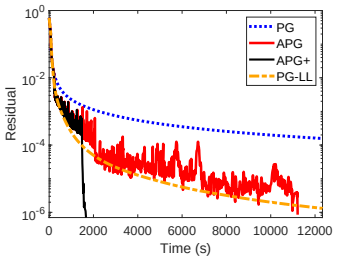

(f) webspam, $s = \lceil 0.01m \rceil$

Figure 3: Sparse regularized logistic loss regression.

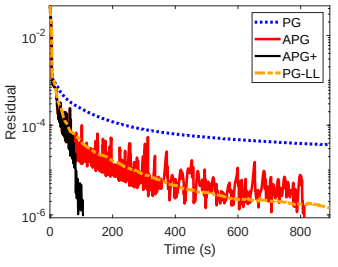

(a) E2006-log1p, $s = \lceil 0.05m \rceil$

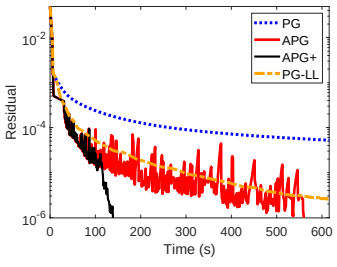

(b) E2006-log1p, $s = \lceil 0.1m \rceil$

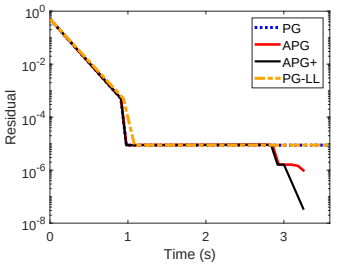

(c) E2006-tfidf, $s = \lceil 0.05m \rceil$

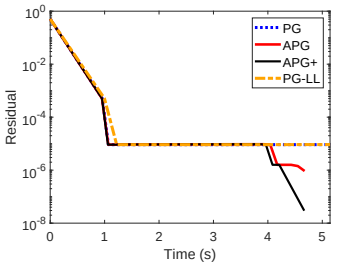

(d) E2006-tfidf, $s = \lceil 0.1m \rceil$

Figure 4: Sparse least squares regression.

Table 4: Comparison of algorithms for (1) to meet (24) with $\hat{\epsilon} < 10^{-6}$, with (23) and (3) and with sparsity level $s_3 = \lceil 0.1m \rceil$ for all datasets except webspam where $s_3 = \lceil 0.01m \rceil$. CPU: CPU time in seconds. GE: number of gradient evaluations. In one iteration, PG, APG, and APG+ needs one gradient evaluation , while PG-LL and PG-LL+ needs two. CG: number of Hessian-vector products in the PCG procedure for obtaining SSN steps. PA: prediction accuracy (for (23)). MSE: mean-squared error (for (3)). Time with $*$ indicates that the algorithm is terminated after running 10000 iterations without satisfying (24).

Dataset	Method	s_3			
		CPU	GE	CG	PA
news20	PG	$*$806.8	10000	0	0.947
	APG	562.7	5972	0	0.927
	APG+	**19.8**	209	133	0.918
	PG-LL	356.6	4578	0	0.930
	APG-LL+	23.2	463	223	0.918
rcv1.binary	PG	$*$81.2	10000	0	0.953
	APG	33.6	2556	0	0.943
	APG+	**2.2**	173	93	0.936
	PG-LL	21.0	2292	0	0.940
	APG-LL+	4.5	542	106	0.933
webspam	PG	$*$42487.5	10000	0	0.980
	APG	11215.1	2242	0	0.993
	APG+	1664.7	313	83	0.994
	PG-LL	14203.9	3176	0	0.992
	APG-LL+	**1565.3**	367	61	0.994
Dataset	Method	s_3			
		CPU	GE	CG	MSE
E2006-log1p	PG	$*$4162.7	10000	0	0.160
	APG	559.9	1084	0	0.142
	APG+	**138.8**	252	122	0.141
	PG-LL	1996.5	4532	0	0.141
	APG-LL+	262.5	601	81	0.139
E2006-tfidf	PG	$*$1086.3	10000	0	0.152
	APG	**4.7**	33	0	0.153
	APG+	**4.7**	31	7	0.139
	PG-LL	512.3	4602	0	0.151
	APG-LL+	8.6	75	7	0.139

Table 5: Comparison of algorithms for (1) to meet (24) with $\hat{\epsilon} = 10^{-6}$, with (23) and (3) and with sparsity levels $s \in \{m, \lceil 1.1m \rceil\}$, i.e. $s \geq m$. CPU: CPU time in seconds. GE: number of gradient evaluations. In one iteration, PG, APG, and APG+ needs one gradient evaluation , while PG-LL and PG-LL+ needs two. CG: number of Hessian-vector products in the PCG procedure for obtaining SSN steps. PA: prediction accuracy (for (23)). MSE: mean-squared error (for (3)). Time with $*$ indicates that the algorithm is terminated after running 10000 iterations without satisfying (24). Time with † indicates that the algorithm is terminated after exceeding 12 hours of running time without satisfying (24).

Dataset	Method	$s = m$				$s = \lceil 1.1m \rceil$			
		CPU	GE	CG	PA	CPU	GE	CG	PA
news20	PG	$*$871.2	10000	0	0.963	$*$869.0	10000	0	0.963
	APG	142.9	1482	0	0.962	191.6	1964	0	0.963
	APG+	58.3	619	24	0.966	**64.8**	684	26	0.969
	PG-LL	156.5	1804	0	0.961	151.8	1778	0	0.961
	APG-LL+	**47.7**	555	9	0.958	66.2	743	9	0.955
rcv1.binary	PG	$*$81.9	10000	0	0.959	$*$82.6	10000	0	0.959
	APG	22.6	1859	0	0.956	18.5	1575	0	0.956
	APG+	5.1	468	47	0.952	5.4	524	47	0.953
	PG-LL	15.7	1780	0	0.955	16.0	1784	0	0.955
	APG-LL+	**4.9**	539	29	0.951	**4.6**	490	38	0.951
webspam	PG	†43206.6	3902	0	0.977	†43203.1	3870	0	0.977
	APG	†43207.8	3866	0	0.985	†43202.0	3852	0	0.982
	APG+	†43207.5	3846	0	0.986	†43210.9	3879	0	0.983
	PG-LL	**35753.0**	3190	0	0.995	**35776.4**	3190	0	0.995
	APG-LL+	36561.7	3190	0	0.995	36494.1	3190	0	0.995
		CPU	GE	CG	MSE	CPU	GE	CG	MSE
E2006-log1p	PG	$*$7039.7	10000	0	0.155	$*$7172.7	10000	0	0.155
	APG	4588.4	5819	0	0.207	5011.5	6275	0	0.213
	APG+	**1050.0**	1362	169	0.344	1320.0	1696	172	0.375
	PG-LL	2261.4	3046	0	0.238	2292.0	3040	0	0.238
	APG-LL+	1220.1	1725	171	0.380	**1282.3**	1751	111	0.340
E2006-tfidf	PG	$*$1821.0	10000	0	0.152	$*$1819.9	10000	0	0.152
	APG	**67.4**	353	0	0.155	**69.0**	363	0	0.155
	APG+	67.8	351	8	0.151	69.4	361	8	0.151
	PG-LL	906.8	4832	0	0.151	909.6	4836	0	0.151
	APG-LL+	69.3	370	8	0.148	72.8	384	0	0.154

Table 6: Comparison of algorithms for (1) to meet (24) with $\hat{\epsilon} = 10^{-6}$, with (23) and (3) and with sparsity levels $s \in \{\lceil 1.5m \rceil, \lceil 2m \rceil\}$, i.e. $s > m$. CPU: CPU time in seconds. GE: number of gradient evaluations. In one iteration, PG, APG, and APG+ needs one gradient evaluation , while PG-LL and PG-LL+ needs two. CG: number of Hessian-vector products in the PCG procedure for obtaining SSN steps. PA: prediction accuracy (for (23)). MSE: mean-squared error (for (3)). Time with $*$ indicates that the algorithm is terminated after running 10000 iterations without satisfying (24). Time with † indicates that the algorithm is terminated after exceeding 12 hours of running time without satisfying (24).

Dataset	Method	$s = \lceil 1.5m \rceil$				$s = \lceil 2m \rceil$			
		CPU	GE	CG	PA	CPU	GE	CG	PA
news20	PG	$*$885.0	10000	0	0.964	$*$904.5	10000	0	0.966
	APG	208.2	2072	0	0.964	217.1	2170	0	0.964
	APG+	78.3	826	17	0.967	86.4	875	18	0.967
	PG-LL	155.8	1736	0	0.963	153.1	1700	0	0.963
	APG-LL+	**64.6**	690	6	0.962	**80.4**	846	2	0.962
rcv1.binary	PG	$*$84.8	10000	0	0.959	$*$87.8	10000	0	0.959
	APG	19.6	1554	0	0.954	15.9	1317	0	0.955
	APG+	**4.4**	412	42	0.953	**4.7**	442	59	0.949
	PG-LL	16.2	1784	0	0.956	16.6	1786	0	0.956
	APG-LL+	4.7	512	22	0.952	5.5	562	14	0.952
webspam	PG	†43201.3	3809	0	0.977	†43207.9	3807	0	0.977
	APG	†43203.8	3815	0	0.978	†43201.7	3792	0	0.983
	APG+	†43202.7	3828	0	0.978	†43205.0	3783	0	0.983
	PG-LL	**36340.5**	3190	0	0.995	36325.1	3190	0	0.995
	APG-LL+	36380.0	3190	0	0.995	**31177.7**	2716	24	0.995
		CPU	GE	CG	MSE	CPU	GE	CG	MSE
E2006-log1p	PG	$*$7617.3	10000	0	0.154	$*$8003.0	10000	0	0.154
	APG	5686.2	6781	0	0.209	6375.8	7300	0	0.201
	APG+	1697.5	2104	118	0.279	2098.5	2496	108	0.280
	PG-LL	2398.6	3002	0	0.231	2460.1	2946	0	0.225
	APG-LL+	**1362.7**	1744	94	0.313	**1672.1**	2057	101	0.299
E2006-tfidf	PG	$*$1870.2	10000	0	0.152	$*$1894.5	10000	0	0.152
	APG	89.0	465	0	0.155	97.0	500	0	0.155
	APG+	89.5	463	8	0.153	97.2	498	8	0.155
	PG-LL	927.8	4848	0	0.151	948.6	4856	0	0.151
	APG-LL+	**72.8**	382	8	0.151	**75.0**	390	8	0.153

Table 7: Comparison of algorithms for (1) to meet (24) with $\hat{\epsilon} = 10^{-6}$, with (3) with sparsity levels $s \in \{\lceil 0.01m \rceil, \lceil 0.05m \rceil, \lceil 0.1m \rceil, \lceil 0.5m \rceil\}$. CPU: CPU time in seconds. GE: number of gradient evaluations. In one iteration, PG, APG, and APG+ needs one gradient evaluation , while PG-LL and PG-LL+ needs two. CG: number of Hessian-vector products in the PCG procedure for obtaining SSN steps. MSE: mean-squared error (for (3)). Time with $*$ indicates that the algorithm is terminated after running 10000 iterations without satisfying (24).

Dataset	Method	$s = \lceil 0.01m \rceil$				$s = \lceil 0.05m \rceil$			
		CPU	GE	CG	MSE	CPU	GE	CG	MSE
colon-cancer	PG	0.44	2081	0	1.125	0.77	3162	0	0.645
	APG	**0.01**	5	0	1.125	0.14	185	0	0.645
	APG+	**0.01**	5	0	1.125	**0.01**	8	3	0.645
	PG-LL	0.21	664	0	1.125	0.19	768	0	0.645
	APG-LL+	**0.01**	10	0	1.125	**0.01**	16	2	0.646
duke	PG	$*$4.07	10000	0	1.568	$*$4.18	10000	0	1.145
	APG	**0.01**	5	0	1.581	**0.01**	8	0	1.140
	APG+	**0.01**	5	0	1.581	**0.01**	8	2	1.140
	PG-LL	0.19	382	0	1.579	0.75	1514	0	1.141
	APG-LL+	**0.01**	10	0	1.581	**0.01**	16	2	1.140
gisette_scale	PG	$*$13.35	10000	0	0.465	$*$14.70	10000	0	0.304
	APG	4.08	1526	0	0.464	3.63	1286	0	0.303
	APG+	**0.07**	11	18	0.464	**0.08**	13	38	0.334
	PG-LL	2.45	1758	0	0.466	$*$30.15	20000	0	0.268
	APG-LL+	**0.07**	32	18	0.464	**0.08**	37	23	0.337
leukemia	PG	3.67	8768	0	0.595	2.80	6726	0	0.566
	APG	**0.01**	5	0	0.595	**0.01**	8	0	0.566
	APG+	**0.01**	5	0	0.595	**0.01**	8	2	0.566
	PG-LL	0.14	302	0	0.595	0.77	1632	0	0.566
	APG-LL+	**0.01**	10	0	0.595	**0.01**	16	2	0.566

Dataset	Method	$s = \lceil 0.1m \rceil$				$s = \lceil 0.5m \rceil$			
		CPU	GE	CG	MSE	CPU	GE	CG	MSE
colon-cancer	PG	1.59	6951	0	0.652	$*$2.51	10000	0	1.855
	APG	0.13	320	0	0.599	1.48	3268	0	2.461
	APG+	**0.01**	10	10	0.599	**0.02**	18	27	1.345
	PG-LL	0.52	2990	0	0.656	$*$6.26	20000	0	1.895
	APG-LL+	**0.01**	24	10	0.599	**0.02**	61	31	1.723
duke	PG	$*$4.28	10000	0	0.860	$*$4.18	10000	0	0.864
	APG	0.02	23	0	0.882	1.26	1749	0	0.569
	APG+	**0.01**	9	5	0.882	**0.01**	11	14	1.060
	PG-LL	0.84	1670	0	0.880	1.05	2284	0	1.089
	APG-LL+	0.02	19	5	0.882	**0.01**	28	14	1.060
gisette_scale	PG	$*$15.63	10000	0	0.243	$*$23.63	10000	0	0.220
	APG	7.83	2697	0	0.212	14.97	3922	0	0.292
	APG+	**0.08**	13	41	0.260	**0.22**	43	108	0.253
	PG-LL	5.37	3294	0	0.238	$*$50.85	20000	0	0.364
	APG-LL+	0.09	54	40	0.259	0.48	271	149	0.258
leukemia	PG	$*$4.35	10000	0	0.523	$*$4.47	10000	0	0.582
	APG	0.99	1263	0	0.524	0.63	876	0	1.277
	APG+	**0.01**	9	5	0.524	**0.01**	10	16	1.676
	PG-LL	0.93	1966	0	0.524	$*$9.79	20000	0	1.226
	APG-LL+	**0.01**	19	5	0.524	**0.01**	30	16	1.676

Table 8: Comparison of algorithms for (1) to meet (24) with $\hat{\epsilon} = 10^{-6}$, with (3) with sparsity levels $s \in \{m, \lceil 1.1m \rceil, \lceil 1.5m \rceil, 2m\}$. CPU: CPU time in seconds. GE: number of gradient evaluations. In one iteration, PG, APG, and APG+ needs one gradient evaluation , while PG-LL and PG-LL+ needs two. CG: number of Hessian-vector products in the PCG procedure for obtaining SSN steps. MSE: mean-squared error (for (3)). Time with $*$ indicates that the algorithm is terminated after running 10000 iterations without satisfying (24).

Dataset	Method	$s = m$				$s = \lceil 1.1m \rceil$			
		CPU	GE	CG	MSE	CPU	GE	CG	MSE
colon-cancer	PG	$*$2.45	10000	0	3.161	$*$2.61	10000	0	3.048
	APG	1.78	3272	0	2.994	0.52	1564	0	3.311
	APG+	**0.03**	39	169	10.643	**0.02**	26	100	6.470
	PG-LL	1.08	5614	0	4.905	3.87	13116	0	4.510
	APG-LL+	**0.03**	192	128	12.519	0.03	137	101	5.062
duke	PG	$*$4.18	10000	0	0.554	$*$4.25	10000	0	0.549
	APG	1.42	1945	0	1.531	1.24	1631	0	0.505
	APG+	**0.01**	13	58	0.209	**0.01**	11	39	2.061
	PG-LL	1.80	3782	0	0.635	1.47	3104	0	0.281
	APG-LL+	0.02	101	87	6.685	**0.01**	58	44	0.831
gisette_scale	PG	$*$35.83	10000	0	0.226	$*$40.06	10000	0	0.225
	APG	16.50	3326	0	0.298	15.55	3000	0	0.308
	APG+	**0.58**	78	247	0.499	**1.20**	200	203	0.347
	PG-LL	21.09	5364	0	0.367	18.91	4462	0	0.359
	APG-LL+	0.99	330	144	0.341	1.59	449	203	0.508
leukemia	PG	$*$4.22	10000	0	0.649	$*$4.30	10000	0	0.703
	APG	1.05	1202	0	0.967	1.06	1445	0	0.980
	APG+	**0.02**	15	104	4.722	**0.02**	17	98	9.202
	PG-LL	$*$9.64	20000	0	1.050	1.87	3968	0	1.718
	APG-LL+	**0.02**	118	104	4.722	**0.02**	112	98	9.202

Dataset	Method	$s = \lceil 1.5m \rceil$				$s = 2m$			
		CPU	GE	CG	MSE	CPU	GE	CG	MSE
colon-cancer	PG	$*$2.71	10000	0	3.277	2.03	8195	0	3.062
	APG	0.27	805	0	2.836	0.22	614	0	3.016
	APG+	**0.02**	27	79	3.092	**0.02**	42	44	3.131
	PG-LL	3.52	14734	0	3.016	0.66	3024	0	2.964
	APG-LL+	0.03	139	67	3.279	0.03	123	63	3.032
duke	PG	$*$4.30	10000	0	0.392	$*$4.28	10000	0	0.333
	APG	0.84	1162	0	0.271	0.51	687	0	0.301
	APG+	**0.01**	13	40	0.259	**0.01**	12	33	0.564
	PG-LL	1.79	3740	0	0.373	1.49	2990	0	0.539
	APG-LL+	0.02	48	34	0.308	0.02	47	33	0.564
gisette_scale	PG	$*$23.09	10000	0	0.230	$*$23.08	10000	0	0.237
	APG	7.40	2057	0	0.284	5.03	1443	0	0.282
	APG+	**0.52**	118	133	0.339	1.32	357	143	0.319
	PG-LL	7.88	3242	0	0.347	6.98	2860	0	0.328
	APG-LL+	1.15	500	150	0.387	**1.13**	488	128	0.336
leukemia	PG	$*$4.36	10000	0	0.730	$*$4.30	10000	0	0.704
	APG	0.69	865	0	0.694	0.47	574	0	0.619
	APG+	**0.02**	19	53	1.369	**0.01**	12	42	0.944
	PG-LL	1.92	3952	0	1.074	1.38	2862	0	0.714
	APG-LL+	0.03	81	49	1.230	**0.01**	43	29	0.926

Table 9: Comparison of algorithms for (1) to meet (24) with $\hat{\epsilon} = 10^{-6}$, with (23) with sparsity levels $s \in \{\lceil 0.01m \rceil, \lceil 0.05m \rceil, \lceil 0.1m \rceil, \lceil 0.5m \rceil\}$. CPU: CPU time in seconds. GE: number of gradient evaluations. In one iteration, PG, APG, and APG+ needs one gradient evaluation , while PG-LL and PG-LL+ needs two. CG: number of Hessian-vector products in the PCG procedure for obtaining SSN steps. PA: prediction accuracy (for (23)). Time with $*$ indicates that the algorithm is terminated after running 10000 iterations without satisfying (24).

Dataset	Method	$s = \lceil 0.01m \rceil$				$s = \lceil 0.05m \rceil$			
		CPU	GE	CG	PA	CPU	GE	CG	PA
colon-cancer	PG	1.69	7560	0	0.667	$*$2.64	10000	0	0.833
	APG	**0.01**	12	0	0.667	0.93	1526	0	0.833
	APG+	**0.01**	9	2	0.667	**0.01**	10	8	0.833
	PG-LL	0.06	226	0	0.667	0.40	1728	0	0.833
	APG-LL+	**0.01**	16	2	0.667	0.02	22	8	0.833
duke	PG	$*$4.52	10000	0	0.000	$*$4.72	10000	0	0.500
	APG	**0.01**	11	0	0.000	**0.01**	12	0	0.500
	APG+	**0.01**	8	1	0.000	**0.01**	8	2	0.500
	PG-LL	0.47	958	0	0.000	0.58	1038	0	0.500
	APG-LL+	**0.01**	15	1	0.000	**0.01**	16	2	0.500
gisette_scale	PG	$*$16.11	10000	0	0.839	$*$17.50	10000	0	0.912
	APG	11.62	3600	0	0.888	6.81	1980	0	0.916
	APG+	**0.07**	10	15	0.851	**0.08**	11	23	0.900
	PG-LL	$*$34.11	20000	0	0.863	5.34	2780	0	0.916
	APG-LL+	0.08	29	15	0.851	0.09	38	24	0.898
leukemia	PG	$*$4.60	10000	0	0.824	$*$4.81	10000	0	0.882
	APG	**0.01**	9	0	0.824	0.05	46	0	0.853
	APG+	**0.01**	9	2	0.824	**0.01**	10	6	0.853
	PG-LL	0.81	1612	0	0.824	1.23	2278	0	0.853
	APG-LL+	**0.01**	16	2	0.824	**0.01**	20	6	0.853
Dataset	Method	$s = \lceil 0.1m \rceil$				$s = \lceil 0.5m \rceil$			
		CPU	GE	CG	PA	CPU	GE	CG	PA
colon-cancer	PG	$*$2.48	10000	0	0.833	$*$2.21	10000	0	0.833
	APG	2.51	3651	0	0.833	0.20	255	0	0.833
	APG+	**0.02**	11	12	0.833	**0.02**	14	55	0.833
	PG-LL	$*$5.79	20000	0	0.833	0.29	1376	0	0.833
	APG-LL+	**0.02**	29	15	0.833	**0.02**	58	44	0.833
duke	PG	$*$4.71	10000	0	0.750	$*$4.81	10000	0	0.750
	APG	0.03	33	0	0.500	0.43	431	0	0.750
	APG+	**0.01**	10	8	0.500	**0.01**	11	11	0.750
	PG-LL	1.22	2352	0	0.500	0.99	1800	0	0.750
	APG-LL+	**0.01**	22	8	0.500	0.02	25	11	0.750
gisette_scale	PG	$*$18.31	10000	0	0.928	$*$27.24	10000	0	0.951
	APG	4.79	1329	0	0.934	2.62	608	0	0.960
	APG+	**0.09**	12	42	0.923	0.23	48	34	0.956
	PG-LL	6.40	3190	0	0.936	7.18	2324	0	0.955
	APG-LL+	**0.09**	56	42	0.923	**0.14**	59	45	0.955
leukemia	PG	$*$4.79	10000	0	0.912	$*$4.81	10000	0	0.912
	APG	0.54	522	0	0.824	0.29	304	0	0.882
	APG+	**0.01**	11	10	0.853	**0.01**	11	9	0.912
	PG-LL	1.50	2726	0	0.912	0.92	1698	0	0.912
	APG-LL+	0.02	21	7	0.853	0.02	24	10	0.912

Table 10: Comparison of algorithms for (1) to meet (24) with $\hat{\epsilon} = 10^{-6}$, with (23) with sparsity levels $s \in \{m, \lceil 1.1m \rceil, \lceil 1.5m \rceil, 2m\}$. CPU: CPU time in seconds. GE: number of gradient evaluations. In one iteration, PG, APG, and APG+ needs one gradient evaluation , while PG-LL and PG-LL+ needs two. CG: number of Hessian-vector products in the PCG procedure for obtaining SSN steps. PA: prediction accuracy (for (23)). Time with $*$ indicates that the algorithm is terminated after running 10000 iterations without satisfying (24).

Dataset	Method	$s = m$				$s = \lceil 1.1m \rceil$			
		CPU	GE	CG	PA	CPU	GE	CG	PA
colon-cancer	PG	$*$2.46	10000	0	0.833	$*$2.33	10000	0	0.833
	APG	0.17	369	0	0.833	0.09	118	0	0.833
	APG+	**0.02**	14	34	0.833	**0.02**	19	35	0.833
	PG-LL	0.32	1336	0	0.750	0.34	1364	0	0.750
	APG-LL+	**0.02**	73	37	0.833	**0.02**	53	39	0.833
duke	PG	$*$4.82	10000	0	0.750	$*$4.81	10000	0	0.750
	APG	0.03	31	0	0.750	0.33	351	0	0.500
	APG+	**0.01**	11	9	0.750	**0.01**	11	9	0.750
	PG-LL	0.81	1558	0	0.750	0.80	1540	0	0.750
	APG-LL+	0.02	23	9	0.750	0.02	23	9	0.750
gisette_scale	PG	$*$40.08	10000	0	0.956	$*$42.05	10000	0	0.957
	APG	1.96	366	0	0.960	3.94	668	0	0.957
	APG+	0.61	102	28	0.962	**0.45**	69	35	0.962
	PG-LL	8.03	1862	0	0.962	8.19	1794	0	0.961
	APG-LL+	**0.25**	57	33	0.959	0.92	192	28	0.962
leukemia	PG	$*$4.79	10000	0	0.912	$*$4.75	10000	0	0.912
	APG	0.43	439	0	0.971	0.25	265	0	0.912
	APG+	**0.01**	11	8	0.912	**0.02**	11	8	0.941
	PG-LL	0.83	1538	0	0.912	0.80	1516	0	0.912
	APG-LL+	0.02	22	8	0.912	**0.02**	22	8	0.941

Dataset	Method	$s = \lceil 1.5m \rceil$				$s = 2m$			
		CPU	GE	CG	PA	CPU	GE	CG	PA
colon-cancer	PG	$*$2.69	10000	0	0.833	$*$2.39	10000	0	0.833
	APG	0.09	219	0	0.667	0.23	304	0	0.833
	APG+	**0.02**	28	25	0.833	0.03	40	20	0.833
	PG-LL	0.37	1282	0	0.833	0.30	1298	0	0.833
	APG-LL+	**0.02**	47	33	0.750	**0.02**	55	25	0.750
duke	PG	$*$4.80	10000	0	0.750	$*$4.83	10000	0	0.750
	APG	0.04	43	0	0.750	0.11	104	0	0.750
	APG+	**0.01**	11	9	0.750	**0.01**	12	11	0.750
	PG-LL	0.84	1496	0	0.750	0.81	1416	0	0.750
	APG-LL+	0.02	30	6	0.750	0.02	25	11	0.750
gisette_scale	PG	$*$26.10	10000	0	0.956	$*$26.29	10000	0	0.956
	APG	2.55	583	0	0.958	1.53	365	0	0.944
	APG+	**0.48**	107	25	0.960	**0.69**	159	23	0.956
	PG-LL	4.66	1658	0	0.958	4.42	1568	0	0.959
	APG-LL+	0.63	193	15	0.960	0.74	242	12	0.958
leukemia	PG	$*$4.67	10000	0	0.912	$*$4.75	10000	0	0.912
	APG	0.44	435	0	0.971	0.03	36	0	0.941
	APG+	**0.02**	12	11	0.941	**0.01**	12	11	0.941
	PG-LL	0.81	1480	0	0.912	0.78	1406	0	0.941
	APG-LL+	**0.02**	25	11	0.941	0.02	25	11	0.941

C.3 Prediction accuracy for varying residuals

We present in Figure 5 the effect of varying the tolerance level $\hat{\epsilon}$ for the residual (24). We can clearly see that in all cases, the prediction performance of all methods keeps improving up to $\hat{\epsilon} = 10^{-5}$, which indicates that our choice of a rather tight stopping condition is indeed a suitable one for getting better prediction performance. Note that in terms of comparison between different algorithms, the results in Figure 5 are consistent with that in Table 1.

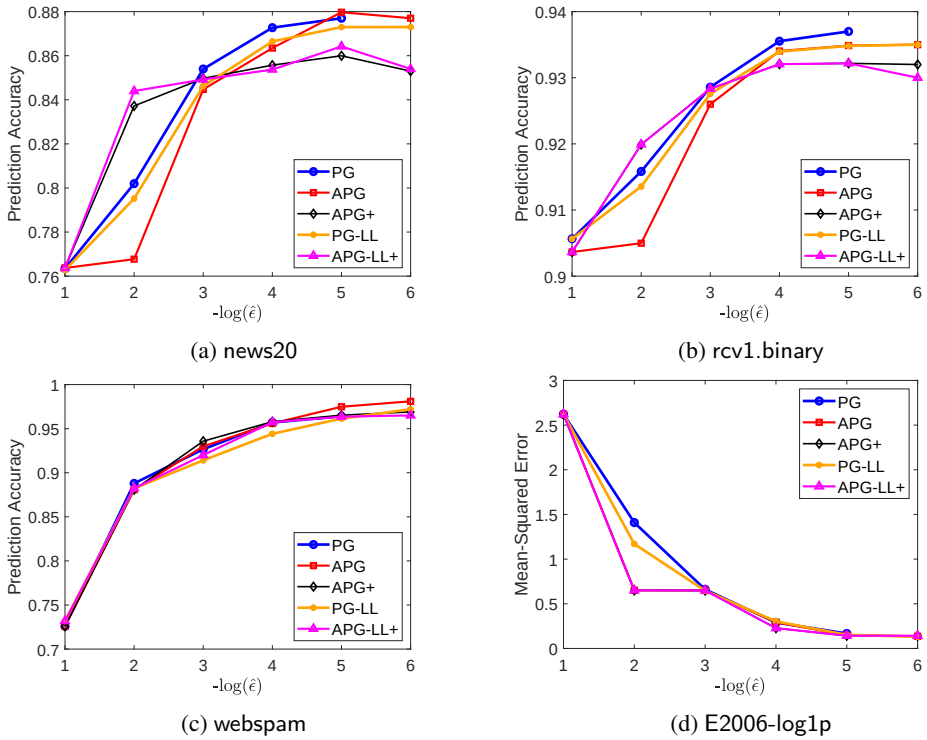

(a) news20 (b) rcv1.binary

(c) webspam (d) E2006-log1p

Figure 5: Prediction performance of different methods for sparse logistic regression (news20, rcv1.binary, webspam) and least squares regression (E2006-log1p) across varying levels of residuals $\epsilon = 10^{-k}$, with $k = 1, 2, \ldots, 6$. Generated plots correspond to sparsity level of $s = \lceil 0.01m \rceil$.

C.4 Numerical comparison with a greedy method

We present in Figure 6 results of numerical comparisons of our methods with the GraSP algorithm of Bahmani et al. [3], which is designed to solve our target problem (1) for general loss functions f. Each iteration of GraSP involves a restricted minimization problem along a subspace of dimension at most $3s$, which is solved by a quasi-Newton approach.[6] Note that GraSP is not ideal for large-scale datasets for its prohibitive memory consumption. For instance, it failed to fit the webspam dataset even with the smallest sparsity level $s = \lceil 0.001m \rceil$ on our machine with 64GB memory with an out of memory error, whereas our proposed algorithm performs quite well for this instance. For a medium-sized dataset such as news20, we see from Figure 6 that GraSP performs significantly slower than our proposed accelerated algorithm. In particular, its initial convergence is extremely fast, but it then becomes stagnant after reaching a low-to-medium precision.

[6] We use their code for regularized sparse logistic regression downloaded from `https://sbahmani.ece.gatech.edu/GraSP.html`.

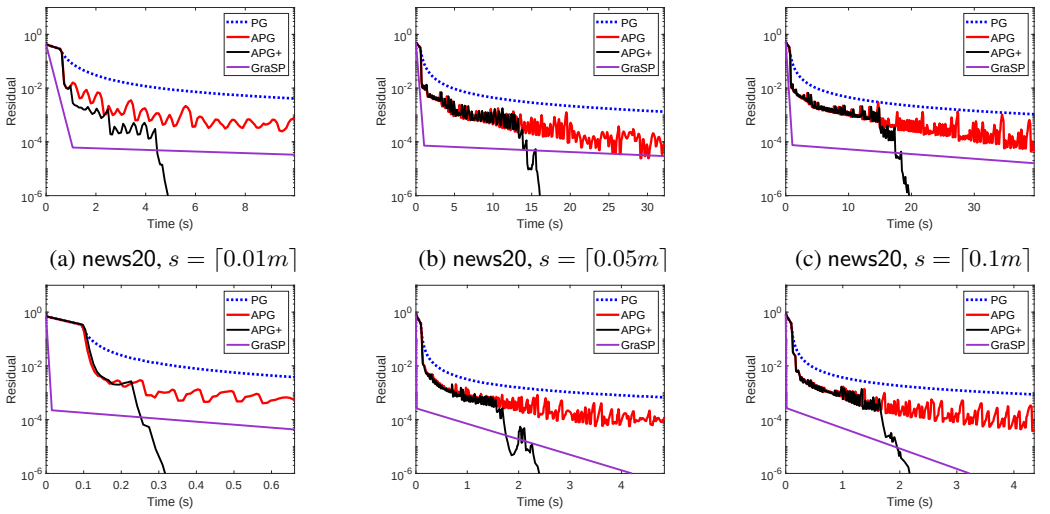

(a) news20, $s = \lceil 0.01m \rceil$ (b) news20, $s = \lceil 0.05m \rceil$ (c) news20, $s = \lceil 0.1m \rceil$

(d) rcv1.binary, $s = \lceil 0.01m \rceil$ (e) rcv1.binary, $s = \lceil 0.05m \rceil$ (f) rcv1.binary, $s = \lceil 0.1m \rceil$

Figure 6: Comparison of non-accelerated and accelerated projected gradient methods with GraSP for solving regularized sparse logistic regression.

D Proofs of Results in Section 2

D.1 Proof of Theorem 2.1

Proof of part (a). We note that the iterates of (5) are confined to A_s. Consider any accumulation point w^* of $\{w^k\}$. For any given convergent subsequence $\{w^{k_r}\}$ with $w^{k_r} \to w^*$, we obtain from the finiteness of $\mathcal{J}_s$ that there is $J \in \mathcal{J}_s$ such that

$$w^{k_r+1} = P_{A_J}(w^{k_r} - \lambda \nabla f(w^{k_r})) \tag{28}$$

for infinitely many r. By taking subsequences if necessary, we assume that (28) holds for all r without loss of generality. Meanwhile, the PG iterates (5) can alternatively be written as

$$w^{k+1} \in \arg\min_{y \in A_s} \ \left\langle \nabla f(w^k), y - w^k \right\rangle + \frac{1}{2\lambda}\|y - w^k\|^2. \tag{29}$$

We also use the fact that (6) implies the well-known descent lemma [see for example, 7, Lemma 5.7]

$$f(w) \le f(w') + \langle \nabla f(w'), w - w' \rangle + \frac{L}{2}\|w - w'\|^2, \quad \forall w, w' \in \Re^n. \tag{30}$$

Noting that $\lambda \in (0, L^{-1})$, we have

$$\begin{aligned}
& f(w^{k+1}) \\
\overset{(30)}{\le} \ & f(w^k) + \left\langle \nabla f(w^k), w^{k+1} - w^k \right\rangle + \frac{L}{2}\|w^{k+1} - w^k\|^2 \\
= \ & f(w^k) + \left\langle \nabla f(w^k), w^{k+1} - w^k \right\rangle + \frac{1}{2\lambda}\|w^{k+1} - w^k\|^2 + \left(\frac{\lambda L - 1}{2\lambda}\right)\|w^{k+1} - w^k\|^2 \\
\overset{(29)}{\le} \ & f(w^k) + \left(\frac{\lambda L - 1}{2\lambda}\right)\|w^{k+1} - w^k\|^2.
\end{aligned}$$

That is,

$$\frac{1 - \lambda L}{2\lambda}\|w^k - w^{k+1}\|^2 \le f(w^k) - f(w^{k+1}). \tag{31}$$

If $w^N = w^{N+1}$ for some N, then it is clear from (31) that $w^k = w^N$ for all $k \ge N$. Otherwise, $\{f(w^k)\}$ is strictly decreasing, proving the first claim of part (a). Noting that ∇f and P_{A_J} are continuous as A_J is closed and convex, we obtain from (28) that $w^{k_r+1} \to P_{A_J}(w^* - \lambda \nabla f(w^*))$ as $r \to \infty$. On the other hand, we see from (31) and the lower boundedness of f that $\|w^k - w^{k+1}\| \to 0$, which, by means of the triangle inequality, implies that $w^{k_r+1} \to w^*$. Hence, we have $w^* = P_{A_J}(w^* - \lambda \nabla f(w^*))$. To complete the proof of part (a), we only need to show that $P_{A_J}(w^* - \lambda \nabla f(w^*)) \in P_{A_s}(w^* - \lambda \nabla f(w^*))$. But from (28) and (5), we have that for all r, $w^{k_r} \in D_J$, where

$$D_J := \{z \in \Re^n : \operatorname{dist}(z - \lambda \nabla f(z), A_J) = \operatorname{dist}(z - \lambda \nabla f(z), A_s)\}, \tag{32}$$

where for any point x and any set A, $\operatorname{dist}(x, A)$ is the distance from x to A, defined as

$$\operatorname{dist}(x, A) = \inf_{y \in A} \|x - y\|.$$

Since A_J is closed, it follows that D_J is a closed set as well, and therefore $w^* \in D_J$. That is, $P_{A_J}(w^* - \lambda \nabla f(w^*)) \in P_{A_s}(w^* - \lambda \nabla f(w^*))$, as desired.

Finally, we note that by representing (1) as

$$\min_w \quad f(w) + \delta_{A_s}(w),$$

where δ_{A_s} is the indicator function of A_s that outputs 0 when $w \in A_s$ and infinity otherwise, a point w^* is called stationary for (1) if

$$0 \in \partial f(w^*) + \partial \delta_{A_s}(w),$$

where ∂g is the limiting subdifferential in the sense of Clarke. On the other hand, the optimality condition of $w^* \in P_{A_s}(w^* - \lambda \nabla f(w^*))$ implies that

$$0 \in w^* - (w^* - \lambda \nabla f(w^*)) + \partial \delta_{A_s}(w^*) \quad \Leftrightarrow \quad 0 \in \lambda \nabla f(w^*) + \partial \delta_{A_s}(w^*).$$

Since $\lambda \delta_{A_s} = \delta_{A_s}$ for any λ, the result above further implies that

$$\lambda^{-1} 0 = 0 \in \nabla f(w^*) + \partial \delta_{A_s}(w^*),$$

showing that w^* is indeed a stationary point of (1). □

Proof of part (b). Suppose that $w^k \to w^*$ and define I_{w^*} as in (8). The finiteness of $\mathcal{J}_s$ implies that there exists $\delta > 0$ such that

$$B_\delta(w^*) \cap A_J = \emptyset, \quad \forall J \notin I_{w^*}, \tag{33}$$

where $B_\delta(w^*) \coloneqq \{w \in \Re^n : \|w - w^*\| < \delta\}$. Since $w^k \to w^*$, we can find $N > 0$ such that $w^k \in B_\delta(w^*)$ for all $k \geq N$. Hence, (8) immediately follows.

Now, suppose that $T_{\mathrm{PG}}(w^*)$ is a singleton for some accumulation point w^*. Together with Theorem 2.1 (a), we have

$$P_{A_s}(w^* - \lambda \nabla f(w^*)) = \{w^*\} \tag{34}$$

It is easy to verify that (34) implies that

$$w^* = P_{A_J}(w^* - \lambda \nabla f(w^*)) \quad \forall J \in I_{w^*}. \tag{35}$$

That is, w^* is a global minimum of f over A_J for all $J \in I_{w^*}$ due to the convexity of f. Now let $\delta > 0$ be as defined in the preceding paragraph and $z \in A_s \cap B_\delta(w^*)$. It then follows from (33) that $z \in A_J$ for some $J \in I_{w^*}$. By the global minimality of w^* for $f|_{A_J}$, it follows that $f(w^*) \leq f(z)$ for all $z \in A_s \cap B_\delta(w^*)$. That is, w^* is a local minimum of f over A_s.

It remains to show that the full sequence $\{w^k\}$ converges to w^*. To this end, choose $\nu > 0$ sufficiently small such that $z \in D_J \cap B_\nu(w^*)$ for some J implies $w^* \in D_J$, where D_J is defined as in (32). Note that such a ν exists as the collection $\{D_J : J \in \mathcal{J}_s\}$ is finite and consists of closed sets. Let $\{w^{k_r}\}_{r=0}^\infty$ be a subsequence converging to w^*. We may assume without loss of generality that $w^{k_r} \in B_\nu(w^*)$ for all $r \geq 0$. First, we show that $w^{k_0+1} \in B_\nu(w^*)$. Note that the convexity of f and (6) result to nonexpansiveness of the mapping $w \mapsto w - \lambda \nabla f(w)$ because $\lambda \leq L^{-1}$ [7, Theorem 5.8]. From (5), $w^{k_0+1} = P_{A_J}\left(w^{k_0} - \lambda \nabla f(w^{k_0})\right)$ for some J. By the choice of ν and the fact that $T_{\mathrm{PG}}^\lambda(w^*)$ consists of one element, we see that $w^* = P_{A_J}(w^* - \lambda \nabla f(w^*))$. With these, we have

$$\begin{aligned} \|w^{k_0+1} - w^*\| &= \|P_{A_J}\left(w^{k_0} - \lambda \nabla f(w^{k_0})\right) - P_{A_J}(w^* - \lambda \nabla f(w^*))\| \\ &\leq \|(w^{k_0} - \lambda \nabla f(w^{k_0}) - (w^* - \lambda \nabla f(w^*))\| \qquad (36) \\ &\leq \|w^{k_0} - w^*\| \\ &< \nu, \end{aligned}$$

where (36) follows from the nonexpansiveness of projection mappings onto closed convex sets, while the second inequality follows from the nonexpansiveness of $w \mapsto w - \lambda \nabla f(w)$. Proceeding inductively, we see that $w^k \in B_\nu(w^*)$ for all $k \geq k_0$ and $\{\|w^k - w^*\|\}_{k=k_0}^\infty$ is a decreasing sequence. As its subsequence $\{\|w^{k_r} - w^*\|\}$ converges to zero, it follows that $w^k \to w^*$, as desired. □

Proof of part (c). Note that $w \mapsto w - \lambda \nabla f(w)$ being a contraction implies that there exists $\gamma \in [0, 1)$ such that

$$\|(w^{k_0} - \lambda \nabla f(w^{k_0}) - (w^* - \lambda \nabla f(w^*))\| \leq \gamma \|w^{k_0} - w^*\|. \tag{37}$$

We then obtain the desired inequality (9) by combining (37) and (36). □

D.2 Proof of Theorem 2.2

Proof. We first prove (10). We have from Theorem 2.1 (b) that there exists $N > 0$ such that (8) holds. Moreover, recall from the proof of Theorem 2.1 that

$$w^k \in \operatorname*{arg\,min}_{y \in \Re^n} \quad \left\langle \nabla f(w^{k-1}), y - w^{k-1} \right\rangle + \frac{1}{2\lambda}\|y - w^{k-1}\|^2 + \delta_{A_s}(y), \tag{38}$$

where δ_{A_s} is the indicator function of A_s. If $J_k \in \mathcal{J}_s$ satisfies $w^k \in A_{J_k}$, we can alternatively write (38) as

$$w^k \in \operatorname*{arg\,min}_{y \in \Re^n} \quad Q_{J_k}^{k-1}(y) \coloneqq \left\langle \nabla f(w^{k-1}), y - w^{k-1} \right\rangle + \frac{1}{2\lambda}\|y - w^{k-1}\|^2 + \delta_{A_{J_k}}(y). \tag{39}$$

Recognizing the right-hand side of (39) as a strongly convex function of y, we obtain

$$Q_{J_k}^{k-1}(y) - Q_{J_k}^{k-1}(w^k) \geq \frac{1}{2\lambda}\|y - w^k\|^2, \quad \forall y \in A_{J_k}. \tag{40}$$

Consequently, for any $k \geq N$, we have from (8) that $J_k \in I_{w^*}$ and so $w^* \in A_{J_k}$, which together with (40) implies

$$Q_{J_k}^{k-1}(w^*) - Q_{J_k}^{k-1}(w^k) \geq \frac{1}{2\lambda}\|w^* - w^k\|^2 \quad \forall k \geq N. \tag{41}$$

Meanwhile, by the descent lemma (30) and by noting that $\lambda \in (0, L^{-1})$, we have $f(w^{k-1}) + Q_{J_k}^{k-1}(w^k) \geq f(w^k)$. Thus, for all $k \geq N$,

$$\begin{aligned}
\frac{1}{2\lambda}\|w^* - w^k\|^2 &\leq Q_{J_k}^{k-1}(w^*) + f(w^{k-1}) - f(w^k) \\
&\overset{(39)}{=} \left\langle \nabla f(w^{k-1}), w^* - w^{k-1} \right\rangle + \frac{1}{2\lambda}\|w^* - w^{k-1}\|^2 + f(w^{k-1}) - f(w^k) \\
&\leq f(w^*) - f(w^k) + \frac{1}{2\lambda}\|w^* - w^{k-1}\|^2
\end{aligned}$$

where the last inequality holds by the convexity of f. Thus, we have

$$\sum_{j=N+1}^{k} \left(f(w^j) - f(w^*)\right) \leq \frac{1}{2\lambda}\left(\|w^* - w^N\|^2 - \|w^* - w^k\|^2\right). \tag{42}$$

Hence, (10) immediately follows by noting that $\{f(w^k)\}$ is monotonically decreasing, as proved in Theorem 2.1 (a), and applying [24, Lemma 1].

Now we turn to (11). From the convexity of f, we have that

$$f(w^k) - f(w^*) \leq \left\langle \nabla f(w^k), w^k - w^* \right\rangle. \tag{43}$$

By (35), we can easily conclude that

$$(\nabla f(w^*))_J = 0 \quad \forall J \in I_{w^*}. \tag{44}$$

Meanwhile, through (8), there exists N such that for all $k \geq N$, we can find $J_k \in \mathcal{I}_{w^*}$ such that $w^k \in A_{J_k}$. Thus, we see that

$$\left\langle \nabla f(w^*), w^k - w^* \right\rangle = 0, \quad \forall k \geq N, \tag{45}$$

because only entries of $\nabla f(w^*)$ outside $J_k \in I_{w^*}$ could be nonzero, but those entries are identically 0 for both w^k and w^*, that is, $w_i^k = w_i^* = 0$ for all $i \notin J_k$. We therefore proceed on with (43) as follows:

$$\begin{aligned}
f(w^k) - f(w^*) &\overset{(45)}{\leq} \left\langle \nabla f(w^k) - \nabla f(w^*), w^k - w^* \right\rangle \\
&\leq \left\|\nabla f(w^k) - \nabla f(w^*)\right\| \left\|w^k - w^*\right\| \\
&\overset{(6)}{\leq} L\left\|w^k - w^*\right\|^2, \quad \forall k \geq N,
\end{aligned} \tag{46}$$

where the second inequality is from the Cauchy-Schwarz inequality. Finally, (11) is proven by inserting (9) into (46). □

E Proof of Results in Section 3

E.1 Proof of Theorem 3.1

Proof. Note that for any $k \geq 0$, we have from (12) that

$$f(z^k) \leq f(w^k) - \frac{\sigma}{2} t_k^2 \|d^k\|^2, \quad z^k := w^k + t_k d^k, \tag{47}$$

where t_k is defined to be zero if the condition in Line 3 of Algorithm 1 is not satisfied. Analogous to (31), we have from $w^{k+1} \in T_{\mathrm{PG}}^{\lambda}(z^k)$ that

$$\frac{1 - \lambda L}{2\lambda}\|z^k - w^{k+1}\|^2 \leq f(z^k) - f(w^{k+1}). \tag{48}$$

Using (48) together with (47), we have

$$\frac{\sigma}{2}t_k^2\|d^k\|^2 \leq f(w^k) - f(w^{k+1}). \tag{49}$$

Then $\{f(w^k)\}$ is decreasing, and since f is bounded below over A_s, we have

$$t_k^2\|d^k\|^2 \to 0. \tag{50}$$

Now, assume that $\{w^{k_r}\}$ is a subsequence of a sequence generated by Algorithm 1 that converges to w^*, and as in the proof of Theorem 2.1, we assume that there exists $J \in \mathcal{J}_s$ such that

$$w^{k_r+1} = P_{A_J}(z^{k_r} - \lambda\nabla f(z^{k_r})) \tag{51}$$

for all r. Then from (50), we have that $z^{k_r} \to w^*$ so that $w^{k_r+1} \to P_{A_J}(w^* - \lambda\nabla f(w^*))$. Meanwhile, (48) gives $\|z^k - w^{k+1}\| \to 0$, and therefore $w^{k_r+1} \to w^*$. Hence, $w^* = P_{A_J}(w^* - \lambda\nabla f(w^*))$. The rest now follows from exactly the same arguments used in the latter part of the proof of Theorem 2.1 (a). □

E.2 Proof of Theorem 3.2

Proof. We consider the sequence $\{w^0, z^0, w^1, z^1, w^2, z^2, \ldots, w^k, z^k, \ldots\}$ and remove those z^k with $z^k = w^k$ from the sequence, and call the resulting sequence $\{\bar{w}^m\}$. We will show that actually $\bar{w}^m \to w^*$, and since $\{w^k\}$ is a subsequence of $\{\bar{w}^m\}$, its convergence to the same point will ensue. Note that if n_k denotes the number of successful extrapolation steps in the first k iterations of Algorithm 1, then $w^k = \bar{w}^{k+n_k}$. Moreover, it is easy to check that w^* is likewise an accumulation point of $\{\bar{w}^m\}$.

To prove the desired result, we first show that the following properties are satisfied:

(H1) There exists $a > 0$ such that

$$f(\bar{w}^m) \leq f(\bar{w}^{m-1}) - a\big\|\bar{w}^m - \bar{w}^{m-1}\big\|^2 \quad \forall m \in \mathbb{N}. \tag{52}$$

(H2) There exists $b > 0$ such that for all $m \in \mathbb{N}$, there is a vector $v^m \in \partial\delta_{A_s}(\bar{w}^m)$ satisfying

$$\|\nabla f(\bar{w}^m) + v^m\| \leq b\big\|\bar{w}^m - \bar{w}^{m-1}\big\|. \tag{53}$$

To this end, fix $m \in \mathbb{N}$, and we separately consider two cases: $\bar{w}^m = w^k$ for some k and $\bar{w}^m = z^k$ for some k.

Case I: $\bar{w}^m = w^k$.
First, suppose that $\bar{w}^m = w^k$ for some k. Then $\bar{w}^{m-1} \in \{w^{k-1}, z^{k-1}\}$. In either case, we have from (31) or (48) that

$$f(\bar{w}^m) \leq f(\bar{w}^{m-1}) - \frac{1-\lambda L}{2\lambda}\big\|\bar{w}^m - \bar{w}^{m-1}\big\|^2, \tag{54}$$

that is, (52) is satisfied with $a = (1-\lambda L)/(2\lambda)$. On the other hand, since $\bar{w}^m \in T_{\mathrm{PG}}^{\lambda}(\bar{w}^{m-1})$, similar to (39), we have

$$\bar{w}^m = \operatorname*{arg\,min}_{y\in\Re^n} \quad \big\langle\nabla f(\bar{w}^{m-1}), y - \bar{w}^{m-1}\big\rangle + \frac{1}{2\lambda}\|y - \bar{w}^{m-1}\|^2 + \delta_{A_{J_k}}(y), \tag{55}$$

where $J_k \in \mathcal{J}_s$ satisfies $\bar{w}^m = w^k \in A_{J_k}$. From the optimality condition of (55), we have

$$0 \in \nabla f(\bar{w}^{m-1}) + \frac{1}{\lambda}\left(\bar{w}^m - \bar{w}^{m-1}\right) + \partial\delta_{A_{J_k}}(\bar{w}^m). \tag{56}$$

That is,

$$v^m := -\nabla f(\bar{w}^{m-1}) - \frac{1}{\lambda}\left(\bar{w}^m - \bar{w}^{m-1}\right) \in \partial\delta_{A_{J_k}}(\bar{w}^m).$$

From [18, Equation (19)], the above equation implies $v^m \in \partial\delta_{A_s}(\bar{w}^m)$. Moreover,

$$\begin{aligned}\|\nabla f(\bar{w}^m) + v^m\| &= \left\|\nabla f(\bar{w}^m) - \nabla f(\bar{w}^{m-1}) - \frac{1}{\lambda}\left(\bar{w}^m - \bar{w}^{m-1}\right)\right)\right\| \\ &\overset{(6)}{\leq} \left(L + \frac{1}{\lambda}\right)\big\|\bar{w}^m - \bar{w}^{m-1}\big\|,\end{aligned} \tag{57}$$

that is, (53) is satisfied with $b = L + \lambda^{-1}$.

Case II: $\bar{w}^m = z^k$.
We now consider the other possibility that $\bar{w}^m = z^k$, in which case, we necessarily have $\bar{w}^{m-1} = w^k$, $d^k \neq 0$, and $t_k > 0$. By (12), (52) is already satisfied with $a = \sigma$. To prove that (H2) holds, we first bound the final step size t_k in the line search procedure. Using (30), we see that (12) is satisfied if

$$t_k \left\langle \nabla f(w^k), d^k \right\rangle + \frac{t_k^2 L}{2} \left\| d^k \right\|^2 \leq -\sigma t_k^2 \left\| d^k \right\|^2$$

or equivalently, recalling that $t_k > 0$, we have

$$-\left\langle \nabla f(w^k), d^k \right\rangle \geq \left(\frac{L}{2} + \sigma) \right) t \left\| d^k \right\|^2. \tag{58}$$

Therefore, (12) is satisfied whenever

$$\begin{aligned} t_k &\overset{(58)}{\leq} -\frac{\left\langle \nabla f(w^k), d^k \right\rangle}{\left\| d^k \right\|^2 \left(\frac{L}{2} + \sigma \right)} \\ &\overset{d^k \in A_J}{=} -\frac{\left\langle (\nabla f(w^k))_J, (d^k)_J \right\rangle}{\left\| d^k \right\|^2 \left(\frac{L}{2} + \sigma \right)} \\ &\overset{(20)}{=} \frac{\zeta_k \left\| (\nabla f(w^k))_J \right\|}{\left(\frac{L}{2} + \sigma \right) \left\| d^k \right\|}. \end{aligned} \tag{59}$$

By applying the condition of $\zeta_k \geq \epsilon$ to (59), we get that (12) is satisfied whenever

$$t_k \leq \frac{\epsilon \left\| (\nabla f(w^k))_J \right\|}{\left(\frac{L}{2} + \sigma \right) \left\| d^k \right\|}.$$

Therefore, we see that t_k is lower-bounded by

$$\begin{aligned} t_k &\geq \min \left\{ c_k \alpha_{\min}, \frac{\eta\epsilon \left\| (\nabla f(w^k))_J \right\|}{\left(\frac{L}{2} + \sigma \right) \left\| d^k \right\|} \right\} \\ &\overset{(20)}{=} \min \left\{ \frac{\left\| (\nabla f(w^k))_J \right\|}{\zeta_k \left\| d^k \right\|} \alpha_{\min}, \frac{\eta\epsilon \left\| (\nabla f(w^k))_J \right\|}{\left(\frac{L}{2} + \sigma \right) \left\| d^k \right\|} \right\} \\ &\geq \frac{\left\| (\nabla f(w^k))_J \right\|}{\left\| d^k \right\|} \min \left\{ \alpha_{\min}, \frac{\eta\epsilon}{\left(\frac{L}{2} + \sigma \right)} \right\}, \end{aligned}$$

where the factor of η is to consider the possibility of overshooting and the last inequality is from that $\zeta_k \in (0, 1]$ in (20). We thus conclude that for the final update $t_k d^k$, we have

$$\left\| t_k d^k \right\| \geq \left\| (\nabla f(w^k))_J \right\| \underline{t}, \quad \underline{t} \coloneqq \min \left\{ \alpha_{\min}, \frac{\eta\epsilon}{\left(\frac{L}{2} + \sigma \right)} \right\}. \tag{60}$$

We then get from (6) and (60) that

$$\left\| (\nabla f(z^k))_J \right\| \leq \left\| (\nabla f(z^k))_J - (\nabla f(w^k))_J \right\| + \left\| (\nabla f(w^k))_J \right\| \leq (L + \underline{t}^{-1}) \left\| z^k - w^k \right\|. \tag{61}$$

We now furnish the vector required in (H2). Let $v^m \in \partial \delta_{A_s}(\bar{w}^m)$ such that $(v^m)_J = 0$ and $(v^m)_{J^c} \coloneqq -(\nabla f(z^k))_{J^c}$. Then by (61), it is clear that

$$\left\| \nabla f(\bar{w}^m) + v^m \right\| = \left\| (\nabla f(z^k))_J \right\| \leq (L + \underline{t}^{-1}) \left\| \bar{w}^m - \bar{w}^{m-1} \right\|.$$

Setting $a = \min \left\{ (1 - \lambda L)/(2\lambda), \sigma \right\}$ and $b = \max \left\{ L + \lambda^{-1}, L + \underline{t}^{-1} \right\}$, we see that (H1) and (H2) are both satisfied for case I and case II.

The rest of the proof for convergence to w^* will follow from arguments analogous to those used in [2], with the only deviation that our condition (21) is weaker than the KL condition assumed in [2]. Through a careful inspection of the proof of [2, Lemma 2.6,Corollary 2.8], we see that

$$\left(f(\bar{w}^m) - f(w^*) \right)^\theta \leq b\kappa \left\| \bar{w}^m - \bar{w}^{m-1} \right\|, \quad \forall m \in \mathbb{N} \tag{62}$$

is a key inequality for the proof. The above inequality clearly holds when the conventional KL condition holds, and here we will show how (62) will still hold under (21) so all remaining arguments in the proof of [2, Lemma 2.6,Corollary 2.8] ensue to be valid. In either case I or case II above, note that the vector v^m in (H2) has the property that $(v^m)_J = 0$, where $J \in \mathcal{J}_s$ is the index set satisfying $\bar{w}^m \in A_J$. It follows that $(\nabla f(\bar{w}^m))_J$ is a subvector of $\nabla f(\bar{w}^m) + v^m$, so

$$\|(\nabla f(\bar{w}^m))_J\| \leq \|\nabla f(\bar{w}^m) + v^m\|. \tag{63}$$

Using (21), (53), and (63), we immediately obtain (62), as desired. The convergence of the iterates then follows from [2, Theorem 2.9].

As for the rates, we have from (62) and (52) that

$$a(f(\bar{w}^m) - f(w^*))^{2\theta} \leq b^2\kappa^2 \left(f(\bar{w}^{m-1}) - f(\bar{w}^m)\right).$$

That is,

$$aD_m^{2\theta} \leq b^2\kappa^2(D_{m-1} - D_m), \quad D_m \coloneqq f(\bar{w}^m) - f(w^*). \tag{64}$$

We now separately consider different values of θ. One result that is being used repeatedly in our discussion below is that we have from $\bar{w}^m \to w^*$ and the continuity of f that

$$D_m \downarrow 0. \tag{65}$$

Our proof for $\theta \in (1/2, 1)$ is inspired by the proof of Lemma 6 in [34, Chapter 2.2].

(a) When $\theta \in (1/2, 1)$, (64) implies

$$D_m \left(\frac{a}{\kappa^2 b^2} D_m^{2\theta-1} + 1\right) \leq D_{m-1}, \tag{66}$$

and since $2\theta - 1 \in (0, 1)$, (66) leads to

$$D_m^{-(2\theta-1)} \left(1 + \frac{a}{\kappa^2 b^2} D_m^{2\theta-1}\right)^{-(2\theta-1)} \geq D_{m-1}^{-(2\theta-1)}, \tag{67}$$

and we have from (65) that $D_m^{2\theta-1} \downarrow 0$. Therefore, we can find $k_0 \geq 0$ such that

$$\frac{a}{\kappa^2 b^2} D_m^{2\theta-1} < 1, \quad \forall m \geq k_0.$$

As $-(2\theta - 1) \in (-1, 0)$, for $m \geq k_0$ we get

$$\left(1 + \frac{a}{\kappa^2 b^2} D_m^{2\theta-1}\right)^{-(2\theta-1)} \leq 1 + (2^{-2\theta+1} - 1)\frac{a}{\kappa^2 b^2} D_m^{2\theta-1}. \tag{68}$$

By combining (67) and (68), we get that for $m \geq k_0$,

$$D_m^{-(2\theta-1)} - (1 - 2^{1-2\theta})\frac{a}{\kappa^2 b^2} \geq D_{m-1}^{-(2\theta-1)}. \tag{69}$$

We note that for $\theta \in (1/2, 1)$, $2^{-2\theta+1} \in (1/2, 1)$, so

$$C_\theta \coloneqq (1 - 2^{-2\theta+1})\frac{a}{\kappa^2 b^2} > 0.$$

Thus, by summing (69) for $m = k_0 + 1, k_0 + 1, \ldots, k + n_k$ and telescoping, we get

$$D_{k+n_k} \leq \left((k + n_k - k_0)C_\theta + D_{k_0}^{-(2\theta-1)}\right)^{\frac{-1}{2\theta-1}} = O\left((k + n_k)^{\frac{-1}{2\theta-1}}\right),$$

as desired.

(b) When $\theta = 1/2$, we see that (64) reduces to

$$\left(a + b^2\kappa^2\right) D_m \leq b^2\kappa^2 D_{m-1} \quad \Leftrightarrow \quad D_m \leq \frac{b^2\kappa^2}{(a + b^2\kappa^2)} D_{m-1}, \tag{70}$$

which shows a Q-linear convergence rate (as $a > 0$) that directly implies the desired exponential bound.

For $\theta \in (0, 1/2)$, we get $2\theta < 1$, and Thus, by the monotonicity of $\{f(\bar{w}^m)\}$, we can find $k_0 > 0$ such that $D_m \leq 1$ for all $m \geq k_0$. For such m, (64) gets us

$$aD_m \leq aD_m^{2\theta} \leq b^2\kappa^2 \left(D_{m-1} - D_m\right), \quad \forall m \geq k_0,$$

and the same Q-linear rate and exponential bound then follow from (70) and the argument that followed it.

(c) When $\theta = 0$, (64) becomes

$$\frac{a}{\kappa^2 b^2} \leq (D_{m-1} - D_m).$$

Hence, noting that $D_{m-1} - D_m \to 0$ by (65) and $a/(\kappa^2 b^2) > 0$, there must be $k_0 \geq 0$ such that $D_m = 0$ for all $m \geq k_0$.

On the other hand, for the case in which f is convex and $\theta \in (0, 1/2)$, this result follows directly from [25].

□

E.3 Proof of Theorem 3.3

Proof. We will first establish the quadratic convergence of $\{w^{k,j}\}_j$ to w^* when t approaches infinity. The overall quadratic convergence can then be obtained by showing that the iterates will all stay within the same A_J and applying Theorem F.1 in Appendix F.

For the part of $\{w^{k,j}\}_j$ for a given k, we note that since $\nabla^2 f_J(w^*)$ is positive definite and $w^{k,0} \in U \cap A_J$, w_J^* is an isolated global optimum of f_J (as f_J is convex). Moreover, the algorithm in (22) clearly treats coordinates not in J as nonvariables, and thus the whole sequence of $\{w^{k,j}\}_j$ stays in A_J. Therefore, $\{w^{k,j}\}$ converges quadratically to w^* following standard analysis for Newton methods; see, for example, [33, Chapter 3]. To satisfy the conditions of Theorem F.1, we just need to notice that if we group $t \geq 1$ consecutive Newton iterations as the operation T_2, the convergence speed is $2t \geq 2$, so the quadratic convergence assumption is still satisfied. It is also clear that since w^* is stationary for (1), $\nabla f_J(w_J^*) = 0$ and thus w^* is a fixed point for the Newton steps. For (5), clearly these suffice for our usage of Theorem F.1 to reach the conclusion. □

F Superlinear convergence of Algorithm 2

In this section, we state and prove a general result of a two-step superlinear convergence of Algorithm 2 that is similar in spirit to that in [4] to simply assume that we have a superlinearly convergent subroutine. We consider this abstract form to demonstrate the versatility of our framework and to allow full flexibility to accommodate different problem conditions of $f|_{A_J}$, and also to fit various algorithms like inexact damped/regularized (semismooth) Newton or quasi-Newton methods, instead of giving the impression that we are restricted to a certain algorithm.

Theorem F.1. *Assume that we have a mapping $T_1(w)$ such that its generated iterates $\{w^k\}$ with $w^{k+1} \in T_1(w^k)$ converge to a stationary point w^* of* (1) *and*

$$\|\hat{w} - T_1(w^*)\| \leq \|w - w^*\|, \quad \forall \hat{w} \in T_1(w) \tag{71}$$

for all w in a neighborhood U of w^* and in some A_J with J satisfying $J \in \mathcal{I}_{w^*}$, and that there is another mapping T_2 that, when given an initial point $w^0 \in A_J$, generates iterates that are all in A_J and superlinearly convergent to w^* within U for each $J \in \mathcal{I}_{w^*}$ with $T_2(w^*) = w^*$, then the iterates generated by

$$w^{k+1} \in T_2\left(T_1\left(w^k\right)\right) \tag{72}$$

converge to w^* at the same superlinear rate as that of T_2.

Proof. We assume without loss of generality that

$$\|T_2(w) - w^*\| \leq c\|w - w^*\|^{1+\rho} \tag{73}$$

for some $c, \rho > 0$ for all $w \in A_J \cap U$ for all $J \in \mathcal{I}_{w^*}$. Then by (71), and by denoting

$$\hat{w}^{k+1} \in T_1(w^k),$$

as the element in $T_1(w^k)$ leading to w^{k+1}, we obtain

$$\begin{aligned}
\left\|w^{k+1} - w^*\right\| &= \left\|T_2\left(\hat{w}^k\right) - w^*\right\| \\
&\leq c\left\|\hat{w}^k - w^*\right\|^{1+\rho} \\
&= c\left\|T_1(w^k) - w^*\right\|^{1+\rho} \\
&= c\left\|w^k - w^*\right\|^{1+\rho},
\end{aligned}$$

where the the first inequality is from (73). Therefore, the conclusion of the theorem is proven. □